NET PRIMARY PRODUCTIVITY MODEL INTERCOMPARISON ACTIVITY (NPP) By Wolfgang Cramer and the participants* of the "Potsdam '95" NPP model intercomparison workshop

IGBP/GAIM REPORT SERIES
REPORT #5

NET PRIMARY PRODUCTIVITY MODEL INTERCOMPARISON ACTIVITY (NPP)

By Wolfgang Cramer and the participants* of the "Potsdam '95" NPP model intercomparison workshop

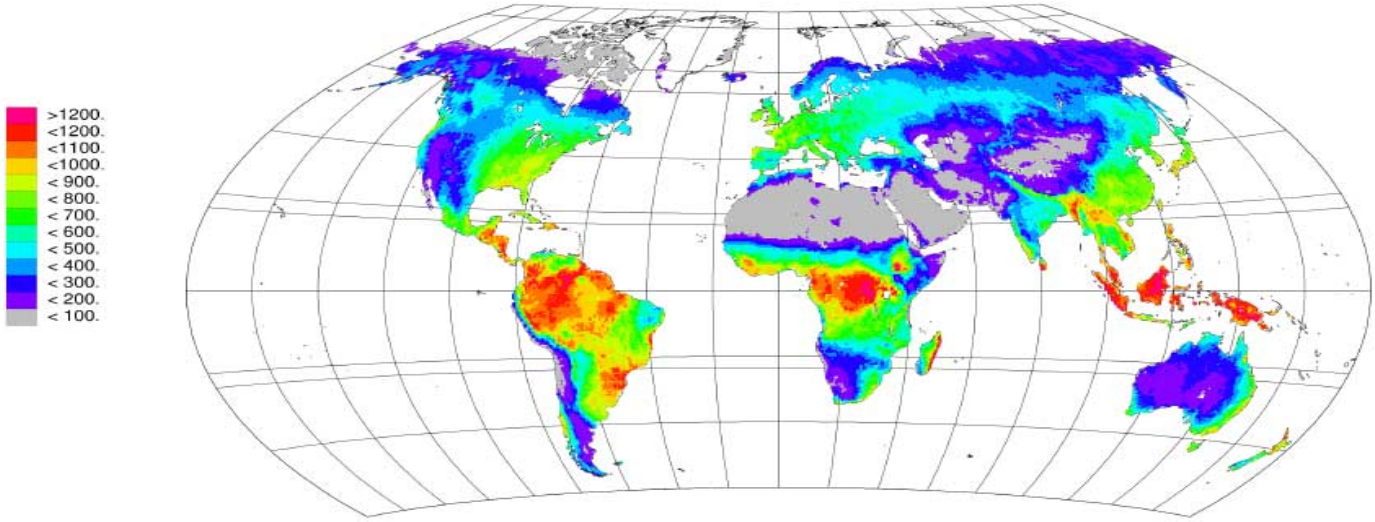

Annual net primary production (g C m^{-2} yr^{-1}) estimated as the average of all model NPP estimates.

- G. Churkina, G. Colinet, J. Collatz, W. Emanuel, G. Esser, C. Field, A. Fischer, A. Friend, A. Haxeltine, M. Heimann, J.Hoffstadt, C. Justice, J. Kaduk, L. Kergoat, D. Kicklighter, W. Knorr, G. Kohlmaier, B. Lurin, P. Maisongrande, P. Martin, R. McKeown, B. Meeson, B. Moore, R. Olson, R. Otto, W. Parton, M. Pleochl, S. Prince, J. Randerson, I. Rasool, B. Rizzo, A. Ruimy, S. Running, D. Sahagian, B. Saugier, A. Schloss, J. Scurlock, W. Steffen, P. Warnant, U. Wittenberg

I G B P
G A I M

Global Analysis, Interpretation and Modelling

Edited by Kathy Hibbard and Dork Sahagian

GLOBAL CHANGE
I G B P

International Geosphere Biosphere Programme

Acknowledgments

The Net Primary Productivity Workshops were made possible by generous support from:

US National Science Foundation (NSF)
US National Aeronautical and Space Administration (NASA)
Potsdam Institute for Climate Impact Research (PIK)

Operating funds for the GAIM office are provided by:
US National Science Foundation (NSF)
US National Oceanographic and Atmospheric Administration (NOAA)
US Department of Energy (DOE)

The enthusiastic participation of all modelling teams in both workshops is gratefully acknowledged. The open spirit of sharing results of ongoing work within the team provided an indispensable basis for the results of the activity. Particularly, the technical support by Blandine Lurin, then at the Paris office of IGBP-DIS, in bringing the data sets together, making them accessible to all participants and performing a range of comparison tasks, is acknowledged. We also thank the computer support group of PIK (Karsten Kramer and Helmut Miethke) for efficient support in running the workshops and managing the database. The scientific sponsorship of this workshop was jointly by GAIM, DIS, and GCTE, and it was hosted by the Potsdam Institute of Climate Impact Research (PIK), with financial support from NASA, the European Commission, and the U.S. Environmental Protection Agency. Visualization and spatial analysis software was supplied for the workshop by Spyglass Inc.

PREFACE

Global Net Primary Productivity (NPP) of ecosystems on land and in the oceans is a crucial component of biogeochemical model development within IGBP. IGBP/GAIM, in conjunction with GCTE and IGBP-DIS has been investigating the performance of terrestrial ecosystem models that treat global NPP. This began with two model intercomparison workshops in 1994 and 1995 at the Potsdam Institute for Climate Impact Research (PIK). The purpose of the workshops was to support a series of model intercomparisons by the various designing teams around the globe that are currently modelling the terrestrial biosphere at large scales with a focus on NPP. The terrestrial carbon cycle models and models that treat energy and water fluxes must address in a fundamental manner either gross primary productivity (GPP) and/or net primary productivity (NPP).

Model intercomparison is necessary for model improvement as part of an iterative process. Primarily, the model output is evaluated by comparison with observations; also, strengths and weaknesses are identified. Next, models are reformulated or parameters are adjusted with the aim of model improvement. Finally, models are run again and the output is re-evaluated. This iterative process is time-consuming and sometimes inefficient. Coordinated model intercomparison can accelerate model improvement because different models perform with varying degrees of success, and the identification of the causes of model strengths and weaknesses is facilitated. In model intercomparisons, the greater the number of models the more fruitful the intercomparison.

There were significant differences in the calculation of NPP within the global terrestrial models compared in 1994, and Potsdam '95 was held in order to compare model parameters and outputs. Financial support for the workshops was provided by NASA, the European Commission, and the U.S. Environmental Protection Agency. Based on the results of model comparisons from the workshops, modelling teams returned to their codes to explore details of model performance. This has resulted in new insights regarding the terrestrial carbon cycle and the function of terrestrial ecosystems. On the basis of these new findings, several papers have been organized into a special issue of "Global Change Biology" featuring Net Primary Productivity, to be published in 1998. This GAIM report summarizes the results of the NPP model intercomparison activity in an attempt to set the stage for future refinement of terrestrial ecosystem models in the context of IGBP.

INTRODUCTION

Future changes in global climate are anticipated as a consequence of the continuing rise in atmospheric CO_2. Predicted climate changes include an increase in mean annual air temperature and alterations in patterns of rainfall and cloud cover [*Houghton et al.*, 1995]. Understanding the response of vegetation to these changes is important because of dependence on plants for food, fuel and lumber. Vegetation also acts as a source, or sink, for the greenhouse gas CO_2. Gross primary productivity (GPP) is the total amount of atmospheric carbon (CO_2) assimilated by vegetation. Net primary productivity (NPP) includes maintenance and growth respiration costs to the plant, and is therefore the net assimilation of atmospheric CO_2 into organic matter. Net primary productivity is driven by solar radiation and can be constrained by light, precipitation and temperature [*Lieth*, 1975]. Other factors such as nutrient availability can also limit the ability of plants to fix carbon. Improved understanding of the biochemistry of photosynthesis has increased our predictive capacity for NPP relative to previous models based on regression techniques, and several mechanistic simulation models of NPP have recently emerged based on the logic introduced by Farquhar et al. (1980). These new mechanistic models generally include one or more environmental controls (e.g. light, water, temperature, nitrogen) on estimates of NPP.

Geographically referenced GPP and NPP and their corresponding seasonal fluctuations are vital to enhance our understanding of both the functioning of living ecosystems and their subsequent feedbacks to the environment. Productivity is also a keystone variable for the sustainability of human use of the biosphere through agriculture and forestry. Recently, it has become possible to investigate the magnitude and geographic distribution of anthropogenic forcings on a global scale by a combination of ecosystem process modelling and monitoring by remote sensing. Since agricultural and forestry production provide the principal food and fuel resources for the world, monitoring and modelling of biospheric primary production are important in order to support global economic and political policy making.

Sufficient data have only recently become available to properly characterize productivity of the terrestrial biosphere. NPP is a quantifiable characteristic of the biosphere and is a fundamental ecosystem variable modeled at the global scale. From a theoretical viewpoint, NPP incorporates most of the annual carbon flux from the atmosphere to the biosphere and is considered to be the main cause of seasonal fluctuations in atmospheric CO_2 concentrations [*Ciais et al.*, 1995; *Keeling et al.*, 1996]. Practical considerations for estimating NPP exist in its utility to measure crop yield, forest production and other economically and socially significant products of vegetation growth.

For estimates of the global carbon balance, a large amount of uncertainty centers on the role of terrestrial ecosystems. Geographically referenced GPP, NPP, heterotrophic respiration (R_h) and their corresponding seasonal variations are key components in the terrestrial carbon cycle. If we are to understand both the function of living ecosystems and their effects on the environment, then we must have a better grasp upon the controls and distribution of GPP, NPP, and R_h. This understanding of biological productivity is pivotal for sustainable human use of the biosphere. To understand the present and to predict the future role of ecosystems in this global context, observations are necessary, but insufficient, and a range of global terrestrial ecosystem models which capture the critical processes in the biosphere are needed. At least two factors

govern the level of terrestrial carbon storage. First, and most obvious, is the anthropogenic alteration of the Earth's surface. An example of this is the conversion of forest to agriculture, which can result in a net release of CO_2 to the atmosphere (e.g. [*Burke et al.*, 1991]. Second, and more subtle, are the possible changes in net ecosystem production (and hence carbon storage) resulting from changes in atmospheric CO_2, other global biogeochemical cycles, and/or the physical climate system. The significant influence of the terrestrial biosphere on the global carbon balance and hence on the problem of climate change has become more widely recognized during the past two decades [*Bolin et al.*, 1979; *Bolin et al*., 1986; *Melillo et al*., 1996; *Moore III et al*., 1981; *Schimel*, 1995a; *Schimel*, 1995b]. Currently, the role of terrestrial ecosystems is recognized to be central to the residence time of carbon dioxide in the atmosphere [*Keeling et al.*, 1996; *Melillo et al.*, 1996; *Moore III and Braswell*, 1994].

In the last few years, a coordinated strategy has been developed to improve estimates of terrestrial net and gross primary productivity through measurement and modelling, primarily through the activities of the IGBP. The strategy has begun to yield dividends: several independent models now exist, others are in various stages of development, and it has become possible to investigate the magnitude and geographical distribution of primary productivity on a global scale by a combination of ecosystem process modelling and monitoring by remote sensing. These models range in complexity from fairly simple regressions between climate variables and one or more estimates of biospheric trace gas fluxes to mechanistic models that attempt to simulate the biophysical and ecophysiological processes occurring at the plant level (including their scaling to large areas). Progress in model development has been significant in recent years, and this development has partly followed similar strategies in different groups. Each approach is based on simplifying assumptions about how ecosystems are structured and how vegetation may respond to changes in various environmental factors. Biospheric flux models all (either explicitly or implicitly) relate geographically specific and comprehensive estimates (and seasonal variations) of temperature, water availability and photosynthetically active radiation (PAR), to some or all of the basic processes of photosynthesis, growth and maintenance respiration, water and nitrogen fluxes, allocation of photosynthates and the production and decomposition of litter.

Among the models participating in the NPP intercomparison, two major groups can be distinguished based on the way they use various data sources. One group is essentially driven by observations made by space-borne sensors, most particularly the National Oceanic/Atmospheric Administration's-Advanced Very High Resolution Radiometer (NOAA-AVHRR). This sensor now provides a relatively long time series and full global coverage with high temporal resolution. These models provide a steadily improved picture of the NPP of the world's actual vegetation. In contrast, other models use data on soils and/or climate alone to derive estimates of the biological activity in the world's potential vegetation (Fig. 1).

One of the early results that emerged from the first NPP model intercomparison workshop was that a major reason for contrasting model results was that the input data were from different sources. This was true for both ground-based observations such as climatic data and for remote sensing data such as the AVHRR-derived Normalized Difference Vegetation Index (NDVI). Consequently, many of these data were standardized for the second workshop. In this exercise, there was a standard database for temperature, precipitation, solar irradiance, and soil texture, a weather generator, AVHRR, and NDVI. Differences still existed in vegetation cover, leaf area index (LAI), and the parameterization of the models for processes such as decomposition, nutrient cycling, and evapotranspiration. Biome definition and distribution has not been successfully standardized throughout the models used in the intercomparison because of differences in approaches, and which may also account for a significant portion of the differences in resulting modeled NPP shown in Figure 2. It was necessary to use as many standardized input data sets as possible in order to make relevant comparisons between modeled NPP formulations.

A fundamental problem of such comparisons is that the target variable, net biospheric carbon flux, cannot be measured at the appropriate spatial scale for any significant part of the globe. Direct validation of any of the models is therefore impractical, although several indirect validation methods exist. Another limitation concerns the quality of the existing observation data sets. For climate, a range of efforts has been made to improve available data sets for the application of biospheric models (including a May, 1996 GCTE/GAIM workshop on that topic). However, climate is only one significant variable. Another one (for potential vegetation) includes soils; for which several activities are currently underway [*Scholes*, 1996]. Two crucial gaps in data exist in the area of historical changes in global land-use, which is clearly a significant element in the world's carbon balance, and in the compilation of point-based observations of biospheric carbon fluxes.

A comprehensive data strategy in support of atmosphere-biosphere interaction models is still lacking. The NPP model intercomparison effort has made it clear that existing data must be chosen and used in a standardized way if similar models are to be compared, and ultimately, if complementary models are to be coupled. It has also clarified data gaps, which can now be filled before models can reliably simulate the role of terrestrial ecosystems in the global carbon cycle. However, it is not necessary for model development to wait until all gaps in the global observing systems are closed. Rather, IGBP can take the lead in coordinating existing and future data sources in a way that will optimize their utility throughout the global change research community.

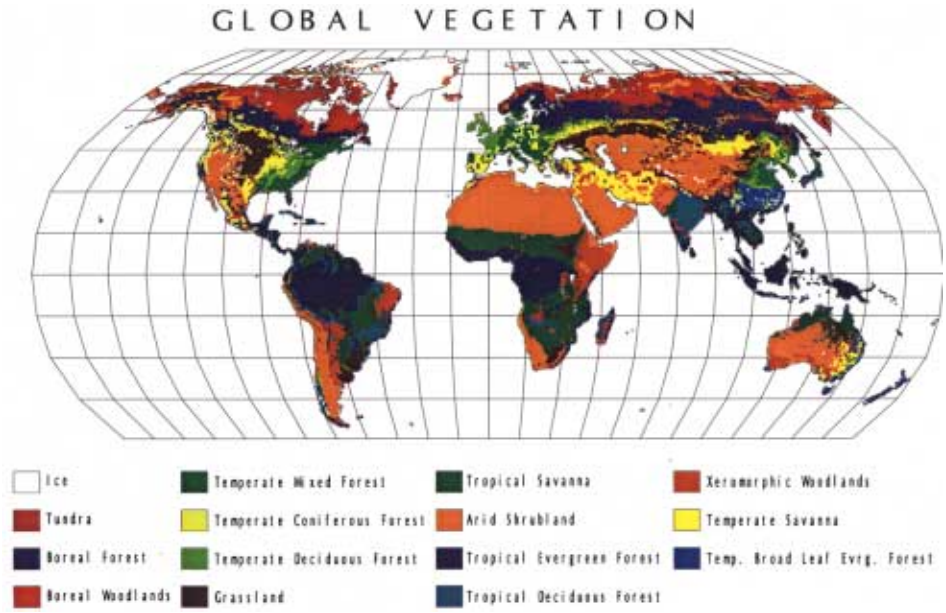

Figure 1: Potential natural vegetation map (modified from Melillo et al. 1993) used for biome-scale comparisons of net primary production among models. Modifications from Melillo et al. (1993) include the aggregation of Arid Shrubland; Short Grassland; and Tall Grassland into Grassland; and Xeromorphic Woodland and Mediterranean Shrubland and Xeromorphic Woodlands.

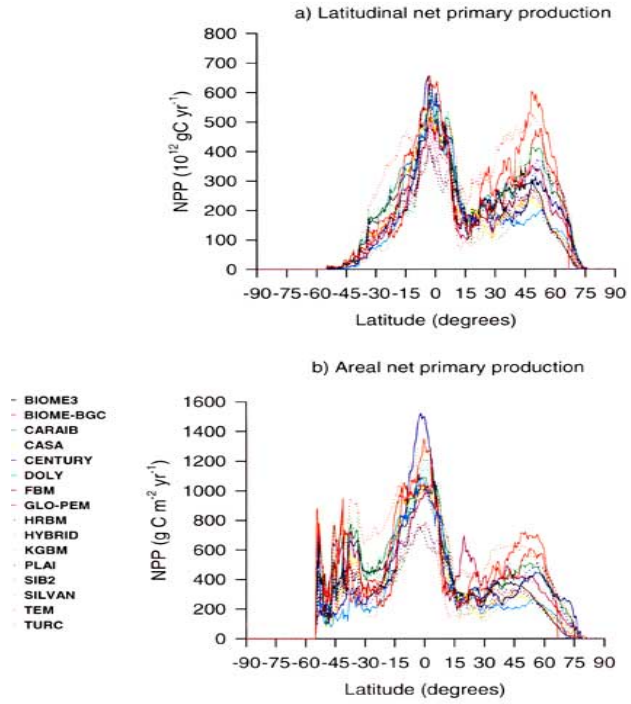

Figure 2: Comparison of the latitudinal distribution of annual net primary production among models either as:

(a) cumulative net primary production (Pg C yr^{-1}) in a 0.5° latitudinal band; or as

(b) mean areal net primary production (g C m^{-2} yr^{-1}) in a 0.5° latitudinal band.

MODELLING APPROACHES

Basic model assumptions

The productivity of the terrestrial biosphere is primarily controlled by the amount of incident radiation and the climatic conditions, i.e. by the meteorological conditions under which plants are able to carry out photosynthesis and then allocate photosynthates to various components. Precipitation and temperature are the two major climatic conditions that govern the absorption of photosynthetically active radiation (PAR) and its conversion into dry matter, i.e. the net primary productivity (NPP) of the biosphere. The pioneer NPP model [*Lieth*, 1975] used an empirical regression to relate annual NPP to the annual average (bio)temperature and precipitation without accounting for radiation. Because of its simplicity and its empirical basis, this model is still used as a baseline for the evaluation and development of more sophisticated mechanistic models.

A large range of more complex models have been developed to account for the ecophysiological and biophysical processes which determine the spatio-temporal features of NPP with a goal of providing prognostic capabilities. Mechanistic relationships are used to describe the fluxes of CO_2 (all models), water (most of the models), and nutrients (few models) between the different compartments of the vegetation, the soil and the atmosphere. The major processes are photosynthesis,

growth and maintenance respiration, evapotranspiration, uptake and release of nitrogen, allocation of photosynthates to the various parts of the plant, litter production and decomposition, and phenological development. Some models focus on detailed mechanistic relationships for some processes (for example, stomatal conductance for water and CO_2 fluxes and net nitrogen mineralization for the nitrogen cycle) and rely on simple empirical relationships or satellite observations to derive or constrain other important features (for example, canopy characteristics, phenology). The seventeen models analyzed in the intercomparison are listed in Table 1, with their key references. The major features of the models are listed in Table 2, and are described below.

To estimate global NPP, ecosystem models are generally driven by input data sets that delineate global climate, vegetation, and soils. In order to compare the methods of estimating NPP between models it is necessary to standardize input data sets, but this is not always practical. For example, a model that requires a known vegetation distribution must use a global vegetation map (or model-based estimate) which is in agreement with its modelling strategy, while others may use different vegetation classes or no map at all. In addition, the input data sets may vary in spatial and temporal resolution so that the resulting NPP estimates also vary in this way (Table 2, columns 2-3).

Table 1: List of participating models, modelling teams and references, listed in alphabetical order.

Model	Full name (if any)	Host Institution	Key references
BIOME3		Department of Ecology, Lund University, Sweden	Haxeltine & Prentice 1996 Haxeltine *et al.* 1996
BIOME-BGC	Biome BioGeochemical Cycles model	School of Forestry, University of Montana, Missoula, MT, USA	Running & Hunt 1993
CARAIB 2.1	CARbon Assimilation In the Biosphere model	Laboratory for Planetary and Atmospheric Physics, Liège University, Liège, Belgium	Warnant *et al.* 1994 Nemry *et al.* 1996
CASA	Carnegie Ames Stanford Approach model	Carnegie Institute of Washington, Stanford University, Stanford, CA, USA	Potter *et al.* 1993 Field *et al.* 1995
CENTURY 4.0		University of Colorado, Fort Collins, Colorado, USA	Parton *et al.* 1993
DOLY		Dept. of Plant and Animal Sciences, Sheffield University, Sheffield, UK & Dept. of Environmental Sciences, University of Virginia, Charlottesville, VA, USA	Woodward *et al*. 1995
FBM 2.2	Frankfurt Biosphere Model	Department of Theoretical and Physical Chemistry, Johann-Wolfgang-Goethe University, Frankfurt/Main, Germany	Kindermann *et al.* 1993 Lüdeke *et al.* 1994 Kohlmaier *et al.* in press
GLO PEM	GLObal Production Efficiency Model	Department of Geography, University of Maryland, MD, USA	Prince 1991 Prince & Goward 1995
HRBM 3.0	High Resolution Biosphere Model	Department of Plant Ecology, Justus-Liebig-University, Gießen, Germany	Esser *et al.* 1994
HYBRID 3.0		Institute of Terrestrial Ecology, Edinburgh, Scotland, UK	Friend 1995 Friend *et al.* 1997
KGBM	Kergoat Global Biosphere Model	Laboratory of Terrestrial Ecology, Toulouse, France	Kergoat in press
PLAI 0.2	Potsdam Land Atmosphere Interaction Model	Potsdam Institute for Climate Impact Research, Potsdam, Germany	Plöchl & Cramer 1995a Plöchl & Cramer 1995b
SDBM	Simple Diagnostic Biosphere Model	Max-Planck Institute for Meteorology, Hamburg, Germany	Knorr & Heimann 1995
SIB2	Simple Interactive Biosphere Model	NASA / Goddard Space Flight Center, Greenbelt, MD, USA	Sellers *et al.* 1996a+b Randall *et al.* 1996
SILVAN 2.2	Simulating Land Vegetation And NPP model	Max-Planck-Institute for Meteorology, Hamburg, Germany	Kaduk & Heimann 1996
TEM 4.0	Terrestrial Ecosystem Model	University of Alaska, Fairbanks, AK, USA The Ecosystems Center, MBL, Woods Hole, MA, USA Complex Systems Research Center, Durham, NH, USA	McGuire *et al.* 1995 McGuire *et al.* in press
TURC	Terrestrial Uptake and Release of Carbon	Carnegie Institute of Washington, Stanford University, Stanford, CA, USA	Ruimy *et al.* 1996

For the Potsdam'95 intercomparison, modelling groups were provided a standard set of climate, soil texture and NDVI data fields. Spatial resolution of the data was a 0.5° by 0.5° Cartesian grid, and the temporal resolution was one month. Data that were used by a small number of models and thus not part of the standardized input data set include wind speed, humidity, spatial distribution and classification of vegetation, biomass, and daily minimum and maximum temperature. Parameterizations based on vegetation and soils were also model-dependent.

NPP was the output variable chosen for a focused evaluation as it was the only variable that was supplied by every model. Noticeable differences occurred for other variables such as gross primary production (GPP), leaf area index (LAI), and simulated, heterotrophic respiration (R_H). At the global scale, input datasets appropriate to initialize models for photosynthetic and respiration processes, soil characteristics, texture and rooting depth, and the availability of nutrients from soils and from litter decomposition may be very limited. The extent to which each process or condition is inferred, modeled or prescribed from literature values differs between models, as does the temporal resolution at which the models operate.

Two basic approaches were used to calculate NPP (Table 2, column 4). Some models (e.g., CASA, CENTURY and HRBM) related NPP directly to vegetation characteristics and environmental variables or indicators such as temperature, precipitation, available soil nitrogen or other fertility factors. Other models estimated NPP as the difference between two processes which were modeled independently: gross primary production (GPP: the total uptake of carbon from the atmosphere by plants), and autotrophic respiration (R_A: the release of carbon to the atmosphere by plant respiration). In the latter case, the environmental and structural variables influenced GPP and R_A instead of NPP.

Table 2: Features of the participating NPP models.

Model	Spatial resolution of NPP	Temporal resolution of NPP	NPP calculated as:	Influenced by	No. of VEGC pools
BIOME3	0.5° x 0.5°	1 month	GPP-R_A	GPP = f(SRad, LAI, Temp, AET/PET, CO_2) R_A = f(LAI, GPP)	0
BIOME-BGC	0.5° x 0.5°	1 day	GPP-R_A	GPP = f(SRad, LAI, Temp, SW, VPD, CO_2, LeafN) R_A = f(VegC, Temp)	4
CARAIB	0.5° x 0.5°	1 day	GPP-R_A	GPP = f(SRad, LAI, Temp, SW, VPD, CO_2, O_2) R_A = f(VegC, LAI, Temp)	2
CASA	1.0° x 1.0°	1 month	NPP	NPP = f(SRad, FPAR, Temp, AET/PET)	0
CENTURY	0.5° x 0.5°	1 month	NPP	NPP = f(VegC, Dead, Temp, SW, Prec, PET, N, P, S)	8
DOLY	0.5° x 0.5°	1 year	GPP-R_A	GPP = f(SRad, LAI, Temp, SW, VPD, CO_2, SoilC&N) R_A = f(VegC, T, SoilC&N)	2
FBM	0.5° x 0.5°	1 day	GPP-R_A	GPP = f(SRad, LAI, Temp, SW, CO_2) R_A = f(VegC, T)	2
GLO-PEM	8 km x 8 km	10 days	GPP-R_A	GPP = f(SRad, fPAR, Temp, SW, VPD) R_A = f(VegC, GPP)	2
HRBM	0.5° x 0.5°	1 month	NPP	NPP = f(Temp, Prec, AET/PET, CO_2, Fert)	0
HYBRID	0.5° x 0.5°	1 day	GPP-R_A	GPP = f(SRad, FPAR, Temp, SW, CO_2, N) R_A = f(VegC, Temp, VegN)	4
KGBM	1.0° x 1.0°	1 day	GPP-R_A	GPP = f(SRad, LAI, Temp, SW, VPD) R_A = f(GPP)	1
PLAI	0.5° x 0.5°	1 day	GPP-R_A	GPP = f(SRad, LAI, Temp, SW, CO_2) R_A = f(VegC, Temp)	2
SDBM	0.5° x 0.5°		NPP	NPP = f(SRad, FPAR, [CO2])	0
SIB2	4.0° x 5.0°	12 minutes	GPP-R_A	GPP = f(Srad, FPAR, LAI, Temp, SW, VPD, CO_2) R_A = f(GPP, Temp, SW)	2
SILVAN	0.5° x 0.5°	6 days	GPP-R_A	GPP = f(SRad, LAI, Temp, AET/PET, CO_2) R_A = f(VegC, Temp)	3
TEM	0.5° x 0.5°	1 month	GPP-R_A	GPP = f(SRad, KLeaf, Temp, AET/PET, CO_2, N) R_A = f(VegC, GPP, Temp)	1
TURC	1.0° x 1.0°	1 month	GPP-R_A	GPP = f(SRad, FPAR) R_A = f(VegC, Temp)	3

The relative influence of different driving variables on NPP varied among the models (Table 2 column 5). Due to the fact that photosynthesis does not occur without sunlight, most models simulated the influence of solar radiation (SRad), and were generally represented through PAR, on NPP. CENTURY and HRBM, however, did not explicitly consider solar radiation. Instead, the influence of solar radiation on NPP was implicitly included in the effects of temperature or self-shading on NPP in these models. Although all models included temperature effects on NPP estimates, the sensitivity of modeled NPP for one or more average climatic variables may not be detectable, particularly when averaged across a zonal or global domain and over an entire year. It was noted, however, that simulated differences in global and zonal NPP may emerge when climatic conditions deviate from average conditions, i.e. interannual time scales. With the exception of the TURC model, all models also simulated the influence of moisture on NPP by incorporating formulations for: (a) soil moisture, (b) soil water potential, (c) vapor pressure deficit; and/or (d) actual or potential evapotranspiration [*Churkina et al.*, 1995]. Maximum potential NPP estimated by CENTURY and HRBM could be reduced by limited nitrogen availability. In BIOME-BGC, DOLY, HYBRID, and TEM, GPP and/or R_A could be constrained by nitrogen availability in the: (a) soil profile, (b) entire vegetation; or (c) leaves only.

Because the storage of carbon in vegetation was represented differently among the models (Table 2, column 6), several approaches were used to estimate GPP, R_A and NPP. For example, some models considered vegetation to be a 'black box' or a single pool of carbon (e.g., TEM) with a single equation describing either GPP, R_A, or NPP. Other models (e.g. BIOME-BGC) divided vegetation carbon into many pools (e.g., leaves, branches, fine and coarse roots) and estimated respiration and the accumulation of carbon, either by GPP or allocation of photosynthates to each pool separately. BIOME3 required the sapwood carbon content in the computation of the respiration costs, and estimated the sapwood pool through the leaf area index (LAI).

Although all models estimated NPP, most of them were primarily developed for other purposes: i) to examine past or future changes in total carbon fluxes and/or storage; or ii) to test hypotheses about the underlying causes of these changes. A review of model structures and input requirements thus shows that certain models may be more appropriate than others to address one scientific question, whereas other models would be more appropriate for other questions. Among the seventeen models in this comparison, three major groups of models were identified based on whether the models use a prescribed seasonal behavior of the radiative activity of the canopy and/or a prescribed vegetation distribution (Table 3). The three categories used three generic approaches to assess the effect of climate on NPP.

Table 3: Categories of participating NPP models, defined on the basis of required input and typical output variables.

Model	Selected inputs			Selected outputs		
Name	Vegetation distribution[a]	Satellite FPAR	Other satellite data[b]	Biogeoche-mical fluxes	Leaf Area Index (LAI)[c]	Vegetation Distribution
A. Satellite based models						
CASA	X	X		X		
GLO-PEM		X	X	X		
SDBM		X		X		
TURC	X	X		X		
SIB2	X	X	X	X		
B. Models for seasonal biogeochemical fluxes						
HRBM				X		
CENTURY	X			X		
TEM	X			X		
CARAIB	X			X	X	
FBM	X			X	X	
PLAI	X			X	X	
SILVAN	X			X	X	
BIOME-BGC	X			X	X	
KGBM	X		X	X	X	
C. Models for seasonal biogeochemical fluxes and vegetation structure						
BIOME3				X	X	X
DOLY				X	X	X
HYBRID				X	X	X

[a] TURC uses biomass data based on Olson et al. (1985). Other models use vegetation types to stratify parameters.

[b] GLO-PEM uses satellite data to estimate photosynthetically active radiation (PAR), surface temperatures, soil moisture, vapor pressure deficit and aboveground biomass. SiB2 uses satellite data to estimate LAI, roughness length and albedo. KGBM uses satellite-derived NDVI data to determine the timing and length of the growing season.

[c] BIOME3 considers foliar projected cover (FPC) instead of LAI.

• The first group of models (category A) required satellite data to determine the temporal behavior of the photosynthetically active component of the canopy. These models could be used to examine the effect of climate variability on NPP, but simulation periods for this class of models are limited to that of the satellite archive [*Kindermann et al.*, 1993; *Kindermann et al.*, 1996; *Maisongrande et al.*, 1995; *Malmstrom et al.*, 1995]. Satellite-driven models have been successfully linked to estimates of terrestrial CO_2 exchanges by an atmospheric transport model with the objective of comparing monthly atmospheric carbon dioxide concentrations that are geographically distributed with respect to sources and sinks of CO_2 [*Heimann and Monfray*, 1989]. For these models, phenology was implicitly prescribed through the use of the seasonal

satellite observations. Note that the distinction between SIB2 and the other satellite-based models is further explained in the "Modelling approaches: Remote sensing based models" section of this paper.

• The second group (category B) simulated the biogeochemical fluxes on the basis of soil and climate characteristics only and by using either spatially explicit vegetation data sets or biogeography models to prescribe vegetation distribution. For HRBM, a prescribed vegetation distribution was needed only for the soil respiration estimates. With one exception, these models simulated phenology either explicitly or implicitly so that the seasonal activity of the canopy could change in response to variable climate. Many of these models have been used to examine the influence of climate change and/or doubled CO2 on NPP [*Melillo et al*., 1993; *Members et al.*, 1995]. However, they simply describe functional changes *within* particular vegetation types. They cannot estimate changes in vegetation distribution as a result of climate change: the vegetation distribution is assumed to remain constant, or they are linked to a biogeography sub-model that assumes a new equilibrium vegetation distribution before the simulation of the new biogeochemical fluxes. The subcategories in Table 3 are based on whether or not the models estimated leaf area index (LAI) and whether LAI was constant or variable over the growing season.

• The third group of models (category C) simulated changes in both ecosystem structure (vegetation distribution and phenology) and function (biogeochemistry). Generally, equilibrium assumptions were made in this group, but these could be adapted so that the models were turned into dynamic global vegetation models (DGVMs). To date, these models have only been applied to potential vegetation so they do not account for land use and its many interactions with climate changes. Some of the models in the other categories account for land use either explicitly (CARAIB) or implicitly through the use of satellite observations. The following sections provide more detail on the different model formulations within each category.

Remote sensing based models

The appearance of global data sets from satellites like the NOAA/AVHRR since the late 1970s has provided new opportunities for the global monitoring of the temporal variation of terrestrial ecosystems. The linkage between vegetation indices such as the Normalized Difference Vegetation Index (NDVI) and the fraction of absorbed photosynthetically active radiation (FPAR) [*Goward and Huemmrich*, 1992; *Kumar and Monteith*, 1981; *Sellers*, 1985; *Sellers*, 1987] predicts the absorbed photosynthetically active radiation (APAR), and is the current technique utilized to link satellite observations to biological productivity on large scales [*Maisongrande et al.*, 1995]. The approach used by the Production Efficiency Models (PEMs) exploits the concept of *light use efficiency* (LUE) for the conversion of APAR to biomass. Several studies have shown that, under ideal conditions, the rate of primary production is linearly related to PAR absorption [*Landsberg*, 1986; *Monteith*, 1977]. Therefore, it was hypothesized that LUE can be regarded as a conservative quantity. Thus,

$P = e \hat{A} FPAR \times PAR$

where:
- P: primary production (gC m^{-2})
- e: light use efficiency (LUE) (gC MJ^{-1})
- FPAR: canopy intercepted fraction of PAR (dimensionless)
- PAR: incident photosynthetically active radiation (MJ m^{-2})

And the integration is made over the growing season, which is defined here by the period when the canopy effectively absorbs PAR. Therefore, the product FPAR x PAR is non zero.

An attractive feature of the concept is its suitability for use with remotely sensed observations, which provide both the timing of the active period and the quantitative values of FPAR. The approximation that the annual photosynthetic activity is a conservative function of APAR permits monitoring of biospheric activity with little need for ancillary information.

However, several studies have indicated that the production rate may vary in the presence of variable environmental conditions and for plants having different photosynthetic pathways and respiration rates [*Jarvis and Leverenz*, 1983; *Prince*, 1991]. Therefore, some models now combine the PEM structure with more classical process based structures considering nutrient cycling and photosynthetic controls to estimate the variability of the LUE (expressed through a production efficiency function). These satellite-based models are sometimes called 'diagnostic', however such a definition may obscure the very different levels of mechanism that are actually accounted for in the description of the effects of the environmental factors on the LUE.

The PEMs analyzed in the intercomparison differed widely with respect to the degree to which they included process descriptions. Some models applied the LUE concept to NPP (CASA, SDBM), others to GPP. In CASA, TURC and SDBM, the potential LUE value was empirically derived, and may be reduced by environmental constraints, whereas GLO-PEM developed a mechanistic model of the LUE value. SDBM considered a potential LUE, which was reduced by a drought factor (AET/PET). The parameterization of SDBM was tuned such that simulated Net Ecosystem Productivity (NEP = NPP -RH), was comparable to observed station data of seasonal atmospheric CO_2 concentrations when predicted values of NEP are carried via an atmospheric transport model [*Heimann*, 1995; *Heimann and Keeling*, 1989]. The spatio-temporal CO_2 features determined by such a simple diagnostic model constrained by both satellite observations and atmospheric CO_2 measurements have been used to validate the more mechanistic models [*Heimann et al.*, in press]. TURC used one constant LUE value for the estimation of the GPP, and applied environmental constraints on R_A. CASA modified the character of the LUE by

incorporating ecological or biogeochemical aspects of the environment to predict carbon storage dynamics. GLO-PEM mechanistically estimated the maximum LUE for the GPP and estimated the environmental factors from satellite data. This model differed from all the others in this comparison in the sense that it did not require any climatic driving variables**.** The climatic factors that influenced the production efficiency were all derived from satellite observations**.** The only use of a climatology in GLO-PEM was to discern the presence of C_3 or C_4 grasses.

SIB2, despite being a remote sensing based model, was not a PEM: fluxes were simulated at the leaf level and then integrated over the canopy. Therefore, the production was not linearly related to canopy APAR through a light use efficiency. It belongs to the soil-vegetation-atmosphere-transfer (SVAT) class of models, which simulate land surface processes in detail and short time steps (minutes), over coarse spatial resolution for implementation in atmospheric general circulation models (GCMs). Critical parameters for SIB2 were supplied from satellite data, including roughness length, albedo, FPAR and LAI. The philosophy driving SIB2 is primarily to simulate the flow of energy and the exchange of water, which are coupled to the exchange of carbon.

Models of seasonal biogeochemical fluxes

One important feature of the models described in the previous section is that the satellite observations are driving input variables. Some of the models in category B use satellite data as well, but only for calibration or prescription of some processes. All these models have the ability to simulate the seasonal biogeochemical fluxes using climate and soil as driving input variables and vegetation distribution for the parameterization of some processes.

HRBM is the direct successor of the empirical MIAMI model [*Lieth*, 1975]. The estimated annual NPP is redistributed to monthly values according to the seasonality of the actual evapotranspiration (AET). NPP is also influenced by land use, soil fertility and CO_2-fertilization. The version analyzed here used the potential vegetation map generated by BIOME1 [*Prentice et al.*, 1992] to initialize major types of vegetation, based on climate.

CENTURY and TEM are the pioneer mechanistic ecosystem models. TEM was the first global, process-based ecosystem model, linking climate and soils data to a water balance estimation algorithm and then using NPP measurements from different sites to calibrate carbon and nitrogen fluxes. The fluxes are parameterized according to phenological indicators, but the canopy structure (e.g. LAI) is not considered explicitly. CENTURY arose from a background that explicitly considered soil carbon and nitrogen pool turnover rates over widely differing time-scales. Both TEM and CENTURY used a vegetation map [*Melillo et al.*, 1993] which was derived from a number of sources including Matthews (1983) to initialize structural and functional model parameters.

CARAIB, FBM, PLAI and SILVAN were similar in the sense that LAI was sensitive to photosynthesis at the leaf level (hourly/daily time step) and they integrate leaf-level CO_2 fluxes to the canopy. Water-limitations were present, but nutrient limits were not. The values of the parameters used in the process representations depended on the ecosystem or on the vegetation types. The ecosystem distributions were derived from the map of potential vegetation by Matthews (1983) for FBM. CARAIB used the map of Wilson & Henderson Sellers (1985), which included five vegetation types (including crops) co-occurring within each grid cell and simulated the processes independently for each of them. The ecosystems considered by PLAI and SILVAN were the potential biomes from BIOME1 [*Prentice et al.*, 1992]. For FBM, PLAI and SILVAN, calibration was performed within each biome so that the components of the carbon balance were fitted to representative literature values. CARAIB used a calibration of productivity for the five vegetation types co-occurring within each grid.

KGBM and BIOME-BGC required similar inputs and derive several output variables by flux integration over the canopy. These models were fundamentally different from CARAIB, FBM, PLAI and SILVAN in three ways. First, the hydrological cycle was a key process in these models and both of them estimated the maximum sustainable LAI from a water balance model—fluxes of water and CO_2 were mechanistically coupled through canopy conductance using the Penman-Monteith equation. Daily feedbacks between the water and carbon cycle drove estimated GPP such that canopy conductance (and hence, assimilation of photosynthates) could be controlled by changes in evapotranspiration. Second, the seasonality of canopy phenology was not climatically driven. The version of BIOME-BGC used for this exercise prescribed phenology, while KGBM used a satellite derived active season [*Moulin et al.*, in press] to determine the period when LAI was zero (in other model versions, BIOME-BGC derives the seasonality of LAI from satellite observations). Third, no production data was used to calibrate these models. The parameterization of processes depended on vegetation classes which distinguish plant functional types (e.g., evergreen vs. deciduous, broad-leaved vs. needle-leaved, C_3 vs. C_4) rather than the biome classes considered in the biogeochemical models previously described (with the exception of CARAIB). For KGBM, the plant functional types were derived from a simplified vegetation map from Matthews (1983); whereas BIOME-BGC used the vegetation structure provided by BIOME1.

Models of process and pattern (function and structure)

BIOME3, DOLY, and HYBRID are designed to simulate ecosystem function (biogeochemical fluxes) *and* structure (vegetation type and structure). The determination of the vegetation types by a particular model followed rules of process optimization (maximization of the NPP according to soils and climate, or maximization of the LAI to satisfy the annual moisture and carbon balances). Like BIOME-BGC and KGBM, these models did not calibrate the results (or the biogeochemical fluxes) to production data. The values of the parameters used in the process representation were chosen from

the literature and were not adjusted. CO_2 fluxes were simulated at hourly/daily time steps and directly coupled with water fluxes. Although the DOLY model calculated GPP on a daily basis, the allocation of carbon to different vegetation pools and the calculation of respiration occur annually so that the DOLY model estimated NPP on an annual basis. Like CARAIB, FBM, PLAI and SILVAN, various strategies were employed to simulate the seasonal variation of the canopy in BIOME3 and HYBRID. HYBRID differed from the others in the sense that it was not an equilibrium model and applies a gap-model strategy at the global scale. Such models appear to be the most adequate candidates for predicting the response of vegetation to climate change because they allow dynamic coupling of the temporal changes of both structure (e.g. LAI) and function (e.g. carbon, water and nutrient fluxes).

METHODS FOR THE COMPARISON

General considerations

At the Potsdam workshops, model comparisons were carried out by a combination of standardized model runs (including common visualization methods), group discussions among the modelling teams to understand the conceptual differences among the models and subsequent analyses by working groups. Absolute standardization of all external data sets, spatial scale assumptions etc. was not achievable for a broad comparison of this type. Some models were designed to operate with different data sets than others, for example—forcing them to using a standard input file would therefore yield misleading results. The goal was for the highest possible level of standardization using: 1) common spatial framework and input data sets; and 2) common visualization tools.

Common data sets

Being climate-driven, all NPP models had data requirements for temperature and moisture availability. With the exception of GLO-PEM (spatial resolution 8 km x 8 km) and SIB2 (4.0° x 5.0°), the models already used climate data sets that were gridded at 0.5° longitude/latitude resolution (approx. 55 km at the equator, but shorter in longitudinal direction towards the poles). Simulations were performed at 0.5° resolution by all models with the exception of GLO-PEM and SIB2 to allow direct comparisons at the workshop. Again, apart from GLO-PEM and SIB2, the models utilized monthly long-term means of climate. Those running at daily time steps usually generated quasi-daily climate data from monthly averages internally. A few models interpolated quasi-hourly climate data for estimating GPP whereas others (e.g., CARAIB, HYBRID) applied weather generators [*Friend*, in press; *Hubert et al.*, in press] to simulate daily variability. The models operating on 0.5^{o} spatial grids used the same land mask and included all land areas except Antarctica, resulting in a global grid containing 62,483 cells. For this land mask, the CLIMATE data base (long term mean 1931-1960, version 2.1, [*Cramer et al.*, in prep; *Leemans and Cramer*, 1991] was provided to the participants for monthly mean temperatures and precipitation values.

Most models required solar radiation, but the formulations for estimating it differed among the models. Those models that estimate radiation from location (latitude) and cloudiness used a gridded estimate of the number of sunshine hour percentages (as a proxy for cloudiness) from the same CLIMATE database [*Otto et al.*, manuscript]. SIB2 was intimately linked with the Colorado State University general circulation model (CSU-GCM), which, relative to the other models, contained a coarser spatial resolution (4° latitude x 5° longitude), and a higher temporal resolution (hourly or less). SIB2 NPP predictions were from these spatial and temporal resolutions.

With the same objective of simplifying the model comparisons, it was suggested that those models that required satellite data for the quantitative prescription of seasonal changes in FPAR use the same data product from the global records of the Advanced Very High Resolution Radiometer (AVHRR): the FASIR dataset for 1987 of the ISLSCP CD-ROM database [*Meeson et al.*, 1995; *Sellers et al.*, 1994]. This dataset consists of monthly NDVI at a spatial resolution of 1° with improved processing compared to the earlier vegetation indices widely used before. The seasonal FPAR required by the satellite-based models was derived from this FASIR-NDVI. However not all satellite-based models were developed using the FASIR data set, and their adaptation to it produced deteriorated results for the comparison. A fundamental problem that emerged was that some models were conceptually developed for different satellite data sets. GLO-PEM, for example, was designed to use satellite data at a higher temporal and spatial resolution (AVHRR Pathfinder) which also integrate other information (e.g. surface temperature, humidity) that are not available from the FASIR data set. Therefore, the results of GLO-PEM analyzed at the Potsdam'95 workshop were neither the optimal values, nor did they correspond to the published results. The results of TURC were also non-optimal, and different from published values, because it was not possible to adjust some relationships for the use of the FASIR data in time for the workshop. Only CASA and SIB2 were designed for the FASIR dataset. In addition, the results available from SDBM are those from the Potsdam'94 workshop, which used another satellite data set. Therefore the outputs of SDBM have generally not been considered in the intercomparison results presented here, apart from in the section covering light interception/light use efficiency and seasonality. Future intercomparisons need to be aware of the fact that standardization of data sets may also create these types of artifacts.

With the exception of GLO-PEM and SIB2, the satellite data used corresponded to the year 1987, while the input climate data used were the 1931-1960 long-term means. The years from 1931-1960 were anomalous in parts of the tropics [*Hulme*, 1992]. The effects of this inconsistency on global NPP were probably limited, but the diagnostic values given to those models combining non-contemporary satellite derived vegetation activity and climate (although highly useful) must be treated cautiously.

Among the data sets that could not be standardized for the intercomparison were average humidity and wind speed, which were required by some models. Vegetation distribution was an input to several models, and the selected maps (or models) affected results both at the levels of model calibration and application. This feature is central to most models—a strict standardization could have removed features that were critical for the individual model design. Furthermore, the models that estimated both fluxes and vegetation structure (BIOME3, DOLY, HYBRID) did not predict identical vegetation distributions. The primary source of soils data came from the FAO Soil Map of the World [*FAO/UNESCO*, 1977], but the interpretations of FAO categories in terms of soil factors were not standardized across models. Some models used the Zobler soil texture translation to field capacity and wilting point. Pan et al. (1996) have recently shown the uncertainty of biosphere models to such different soil data sets.

The input requirements for all models in more detail are presented in Table 4, below. Only input driving variables used to extrapolate simulations across the globe are listed, which suggests that additional variables required at an early stage in the calibration procedure are not presented. For example, FBM and PLAI used soil types [*Fung et al.*, 1987] to compute heterotrophic respiration. The calibration procedure of these models requires that annual NPP equal annual R_H—indicating that NPP cannot be estimated without a soils dataset. Another example is the NDVI time-series data [*Gallo*, 1992] used by SILVAN to calibrate the phenological sub-model applied for temperate deciduous forests.

Table 4: Input variables as they are required by the different models - same order as in Table 2 (data for calibration are not included)

Model	Veget. type		Soil					Atm.		Climate						
	map	climate	type/texture	r. depth	WHC	C, N	elev.	[CO_2]	NDVI	mean T	ΔT	Prec	humidity	solar radiation	net rad.	wind sp.
CASA	a [D&S]		text [FAO/Z]	f(veg)		[Po]		360	m [F87]	m [CL]		m [CL]		m (λ, c[CL])		
GLO-PEM								34Pa	[F87]	10d (Pathf)		*	10d (Pathf)	m (TOMS)		
SDBM			%text [W]	1m	cst				m [G]	m [CL]		m [CL]		m (λ, c[CL])		
TURC									m [F87]	m [CL]				m (λ, c[CL])		
SIB2	a [Ma, K]		text [FAO/Z]	X	f(t)		X	35Pa	m [F87]	h (GCM)		h (GCM)	h (GCM)	h (GCM)		h (GCM)
HRBM		p (B)	t [FAO]		f(t)			340		m [CL]		m [CL]		m (λ, c[CL])		
CENTURY	p [Me]		%text [FAO]	f(veg)	f(text)			340			m [CL]	m [CL]				
TEM	p [Me]		%text [FAO]		f(text,veg)		X	340		m [CL]		m [CL]		m (λ, c[CL])		
CARAIB	a [W&HS]		text [FAO/Z]	f(t,veg)	cst		X	350		d [CL+wg]	d (wg)	d [CL+wg]	d (FC,PWP)	d (λ, c[CL])		
FBM	p [Ma]		text [FAO/Z]	f(text,veg)	f(text,veg)			350		d [CL]	d f(veg)	d [CL]		d (λ, c[CL])		
PLAI		p (B)	text [FAO/Z]		f(text)			350		d [CL]	d f(veg)	d [CL]		d (λ, c[CL])		
SILVAN		p (B)	%text [W]	[W]	cst			340		d [CL]	d [CL]	d [CL]		d (λ, c[CL])		
BIOME-BGC		p (B)	text [FAO/Z]	2m	f([W&HS])		X	340		d [CL]	d (WGEN)	d [CL]	d [R]	d [R]		
KGBM	p [Ma]		text [FAO/Z]	f(veg)	f(text)			340	w [C86]	d [CL]		d [CL]	d vp [S&J]	d (λ, c[CL])	f(SRad)	
BIOME3			text [FAO/Z]	1.5m	f(text)			340		d [CL]		d [CL]		d (λ, c[CL])		
DOLY						[Z,Po]		350		d [CL]		d [CL]	d [L]	d [H]		
HYBRID			cst	f(Soil-C)	f(Soil-C)	[Pa]		280		d (WGEN)	d (WGEN)	d (WGEN)	d (WGEN)	d (WGEN)		

Vegetation type: a: actual vegetation; p: potential vegetation; [*Dorman and Sellers*, 1989; *Kuchler*, 1983; *Matthews*, 1983; *Melillo et al.*, 1993; *Prentice et al.*, 1992; *Wilson and Henderson-Sellers*, 1985], BIOME-BGC assigns functional types to the biomes.

Soil type/texture: t: soil type; text: texture categories; % texture: percents of sand, silt and clay; [FAO]: [*FAO/UNESCO*, 1977]; [*Webb et al.*, 1992; *Wilson and Henderson-Sellers*, 1985; *Zobler*, 1986]

Soil rooting depth: function of soil type (t), vegetation type (veg), soil carbon (Soil-C); [*Webb et al.*, 1992]

Soil water holding capacity (WHC): function of soil type (t), soil texture (text), vegetation type (veg), soil carbon (Soil-C); [*Wilson and Henderson-Sellers*, 1985]

Soil C, N: [*Parton et al.*, 1993; *Post et al.*, 1985; *Post et al.*, 1990; *Zinke et al.*, 1984]

Atmospheric [CO_2]: in ppmv

NDVI: m: monthly, w: weekly; [S87]: ISLSCP-FASIR 1987 [*Los et al.*, 1994]; [G]: 3 years average from Gallo (1992); [C86]: CESBIO 1986 [*Berthelot et al.*, 1994].

Climate: m: monthly inputs required; d: daily inputs available or interpolated; h: hourly inputs; [CL]: monthly mean Temp, DT, Precipitation, Cloudiness, of the standard CLIMATE database; [CL+wg]: daily interpolation using the weather generator of the model; WGEN: Friend (in press); [L]: Leemans, pers. comm.; (GCM): derived from a GCM; (l, c[CL]): derived from latitude and standard cloudiness [*Otto et al.*, manuscript]; (TOMS): satellite PAR estimates [*Dye and Shibasaki*, 1995]; [H] or [R]: microclimate simulator [*Hungerford et al.*, 1989; *Running et al.*, 1987]; vp [S&L] vapor pressure derived from Spangler & Jenne (1990); 10d (Pathfinder): derived from the decadal AVHRR Pathfinder 1987 data set [*Agbu and James*, 1994].

*: GLO-PEM directly estimates the soil moisture from the AVHRR data set, without data requirements on soil and precipitation.

Comparison strategy

The main strategy of the intercomparison was to confront all modelling teams with all input and output data sets from all models, using a visualization tool which allowed comparisons to take place with identical cartographic features (geographic projection, color scales etc.). The first package of data sets, which had been collected from the teams prior to the workshops, was reformatted (Blandine Lurin, IGBP-DIS, Paris) to a standard GIS format and prepared for on-line visualization and analysis on a large screen in the meeting room. Over the course of several days, working groups analyzed these images. In the plenary sessions, results were then presented and discussed with the other groups. Input and output data sets were organized in a consistent data base structure, located at the computing facility of PIK. Access to this data was provided to all participating teams and comparisons were carried out after the workshops as well.

The general global results are discussed in the next section. Five working groups addressed special issues across all models. Their most important results are summarized briefly in later sections. Because the different variables of the common data sets were derived from different sources and have different spatial resolutions, the terrestrial boundaries of the global data sets do not match precisely. After common input data sets had been, where necessary, re-gridded to a spatial resolution of 0.5° x 0.5° longitude/latitude, the various datasets contained: (1) CLIMATE - 62,483; (2) soil texture - 58,440; and (3) FASIR-NDVI - 86,624 grid cells. There were 56,785 common grid cells that contained the data for the NPP results presented in this model intercomparison.

RESULTS AND DISCUSSION

Total annual net primary production

The models estimated global net primary production of the terrestrial biosphere between 39.9 and 80.5 PgC yr^{-1} with a mean of 54.9 PgC yr^{-1}. Table 5 shows the estimated global NPP values for each model in decreasing order. Although considerable effort was made to reduce the variability among modeled NPP estimates through the use of common data sets, these global NPP estimates were still based on different land areas used by the models (Table 5). The area of the terrestrial biosphere varies from 105.6 to 128.7 10^6 km^2, which is around 18 percent of the 128.7 10^6 km^2 represented by the 56,785 grid cells of the common input data sets. This variation is partly the result of (1) missing data—some models did not estimate NPP for some vegetation classes (e.g., FBM did not estimate NPP for desert regions; TEM did not estimate NPP for wetland or floodplain vegetation types); (2) the use of additional data sets that did not exactly match the grid cells used in the common data sets; and (3) for SIB2, the coarse spatial resolution used to calculate NPP. These differences did not appear to have a major influence on global NPP estimates because they were partially compensated by other factors, or because missing regions were those with relatively low productivity.

The two extreme global NPP values estimated by TURC and HYBRID have model-specific explanations. The TURC simulations for Potsdam'95 were made with the FASIR data set without appropriate re-calibration, resulting in an overestimation of the NPP fluxes compared to other published results: 62.3 Pg C yr^{-1} for the reference computation and 71.3 Pg C yr^{-1} when the FASIR data set was used with re-calibration [*Ruimy et al.*, 1996]. The use of FASIR without re-calibration also unrealistically lengthened the growing season. A pre-industrial atmospheric CO_2 of 280 ppmv may be the cause for low global NPP estimates from HYBRID (Andrew Friend, pers. comm.), whereas the other models considered atmospheric CO_2 concentrations between 340 and 360 ppmv (Table 4).

If TURC and HYBRID are put aside, then the range of global NPP variability is reduced from 100% to 50%, a relatively good agreement for the estimation of this poorly understood variable. It is likely that the explicit calibration procedures used by some models are partly responsible for this, and results presented below suggest that the models may indeed be calibrated such that annual global NPP predictions are within 'commonly admitted values'.

The overall ranking of global NPP cannot be explained by any of the specific model features described below (Table 5), and certainly not by basic model-categories (Table 3). Satellite-based models estimated high values of global NPP (GLO-PEM, TURC), but they also estimated low values (CASA, SIB2). The three models which did not estimate GPP (CASA, CENTURY, HRBM) displayed intermediate to low NPP values. It must be noted, however, that four of the six models that applied nutrient constraints on NPP estimated lower global NPP than models that did not incorporate nutrient limitations in their model formulations.

Four of the six models which included a vapor pressure deficit calculation to determine NPP predicted higher global NPP values than those using other methodologies to estimate the influence of moisture on NPP. These results suggest that NPP estimates may be sensitive to the modelling strategy used to simulate the water balance and the effect of water stress on NPP. One of the models using vapor pressure deficit that predicted a lower global NPP (DOLY) also implemented nutrient constraints on NPP.

Table 5: Comparison of annual and monthly NPP of the globe and the factors influencing NPP among sixteen models, ranked in decreasing order of global annual NPP estimates.

Model	NPP (Pg C yr^{-1})	Number of grid cells	Area (10^6 km^2)	Mean length of growing season (months)[a]	Monthly maximum global NPP (Pg C mo^{-1})	Monthly minimum global NPP (Pg C mo^{-1})	Seasonal range in global NPP (Pg C mo^{-1})	Temporal resolution of NPP	Veg[b]	NDVI	Moisture[c]	Nutrient Constraints[d]
TURC	80.5	56785	128.7	10.5	9.1	4.8	4.3	monthly	A	FPAR		
GLO-PEM	66.3	56785	128.7	6.0	7.7	3.4	4.3	monthly	A	FPAR and others	SW/VPD	
CARAIB	65.2	56785	128.7	6.3	8.4	3.8	4.6	daily	A(M)		SW, VPD	
KGBM	62.5	56785	128.7	6.4	9.1	2.8	6.3	daily	P(D)	PHENO	SW, VPD	
BIOME-BGC	62.2	54279	124.0	6.2	8.4	2.9	5.5	daily	P(D)		SW, VPD	Leaf-N
SILVAN	61.1	56785	128.7	6.8	7.7	3.5	4.2	6days	P(D)		AET/PET	
BIOME3	54.2	56785	128.7	7.5	6.6	3.0	3.6	monthly	P(M)		AET/PET	
CENTURY	53.3	50641	116.9	8.3	6.2	2.9	3.3	monthly	P(B)		SW, Prec	N, P, S
FBM	49.9	47807	105.6	7.4	7.5	2.5	5.0	daily	P(B)		SW	
PLAI	49.2	56785	128.7	5.2	6.6	2.0	4.6	daily	P(B)		SW	
CASA	48.9	56785	128.7	9.1	5.8	3.1	2.7	monthly	A(D)	FPAR	AET/PET	
SIB2	47.9	51050	115.7	7.1	8.3	2.2	6.1	12mn	A(D)	FPAR and others	SW, VPD	
DOLY	46.4	56785	128.7	N/A[e]	N/A	N/A	N/A	year	P(D)		SW, VPD	Soil C&N
TEM	46.2	55290	125.6	6.8	6.7	2.4	4.3	monthly	P(B)		AET/PET	N
HRBM	44.3	56785	128.7	6.0	5.6	2.3	3.3	monthly			Prec, AET/PET	Fert
HYBRID	39.9	56785	128.7	5.7	7.0	-1.6	8.6	daily	P(M)		SW	Veg-N, N

[a] A specific month is considered part of the growing season if its NPP estimate is greater than 10% of the maximum monthly NPP estimate of the grid cell.

[b] NPP estimates are based on the assumption that the world is either covered with potential (P) or actual (A) vegetation. Vegetation type may be either an input variable; implicit within the model (e.g. NDVI data only represents actual vegetation); or explicitly simulated by the model. Within a grid cell, the vegetation may be assumed to be represented by a single dominant (D) vegetation type or a mosaic of vegetation case. In the latter case, the model considers either an average parameterization that is biome-dependent (B), or a distinct parameterization for each vegetation type (M).

[c] The effect of soil moisture on NPP may be described either by using precipitation (Prec), soil water (i.e. soil moisture, soil water potential - SW), vapor pressure deficit (VPD), or actual evapotranspiration (AET) and potential evapotranspiration (PET)

[d] Nutrient constraints may be implemented based on a soil fertility factor (Fert), on the carbon and nitrogen content of soil organic matter (Soil C&N), on the nitrogen content of leaves (Leaf-N), the nitrogen content of both leaves and roots (Veg-N), and/or on inorganic nitrogen (N), phosphorus (P), or sulfur (S) concentrations in the soil.

[e] N/A is not applicable because DOLY estimates only annual NPP

[*Esser and Lautenschlager*, 1994; *Field et al.*, 1995; *Friend and Cox*, 1995; *Friend et al.*, 1997; *Haxeltine and Prentice*, 1996; *Haxeltine et al.*, 1996; *Kaduk and Heimann*, 1996; *Kergoat*, in press; *Kindermann et al.*, 1993; *Knorr and Heimann*, 1995; *Kohlmaier et al.*, 1997; *Ludeke et al.*, 1994; *McGuire et al.*, 1995; *McGuire et al.*, in press; *Nemry et al.*, 1996; *Parton et al.*, 1993; *Plochl and Cramer*, 1995a; *Plochl and Cramer*, 1995b; *Potter et al.*, 1993; *Prentice and III*, 1996; *Prince*, 1991; *Prince and Goward*, 1995; *Randall et al.*, 1996; *Ruimy et al.*, 1996; *Running and Hunt*, 1993; *Sellers et al.*, 1996a; *Sellers et al.*, 1996b; *Warnant et al.*, 1994; *Woodward et al.*, 1995]

Figure 3 shows the global map of annual NPP, averaged across all models. The highest productivity (> 1200 g C m^{-2} y^{-1}) is found in tropical biomes (Amazonia, Central Africa, Southeast Asia), where both temperature and precipitation requirements were fully satisfied for photosynthesis. Temperate regions had an intermediate NPP (500 - 700 g C m^{-2} y^{-1}), and the lowest NPP (< 200 g C m^{-2} y^{-1}) was found in cold or arid regions, where either temperature or precipitation were limiting. The intertropical band in Africa contained the highest spatial variability, from the most productive biomes (tropical evergreen forest) near the equator to the least productive ones (arid shrublands) around latitudes 20 - 25°N.

The variation in NPP estimates among the models reflected the distribution of NPP. The map of the standard deviation of the individual model estimates from the combined model mean (Figure 4a) suggests that the standard deviation is larger where NPP was high and smaller where NPP was low. The highest standard deviation occurred at the borders of areas with high NPP values. This may partially be an artifact due to the different vegetation data sets, which were used as input. In contrast, the highest coefficient of variance was below 15%. In the areas of tropical forests and boreal forests, the coefficient of variation could be less than 5%. However, the coefficient of variance (Figure 4b) was less than 15% for most areas—it was therefore possible to consider the broad features of this figure as a comprehensive representation of NPP fluxes estimated similarly by different models.

The global NPP estimates of all the models varied seasonally (Fig 5). Because most of the terrestrial biosphere is found in the Northern Hemisphere (74% of the global land area, excluding Antarctica), the monthly global NPP estimates of all models were low during the Northern Hemisphere's winter and high during its summer, but the seasonal pattern and magnitude

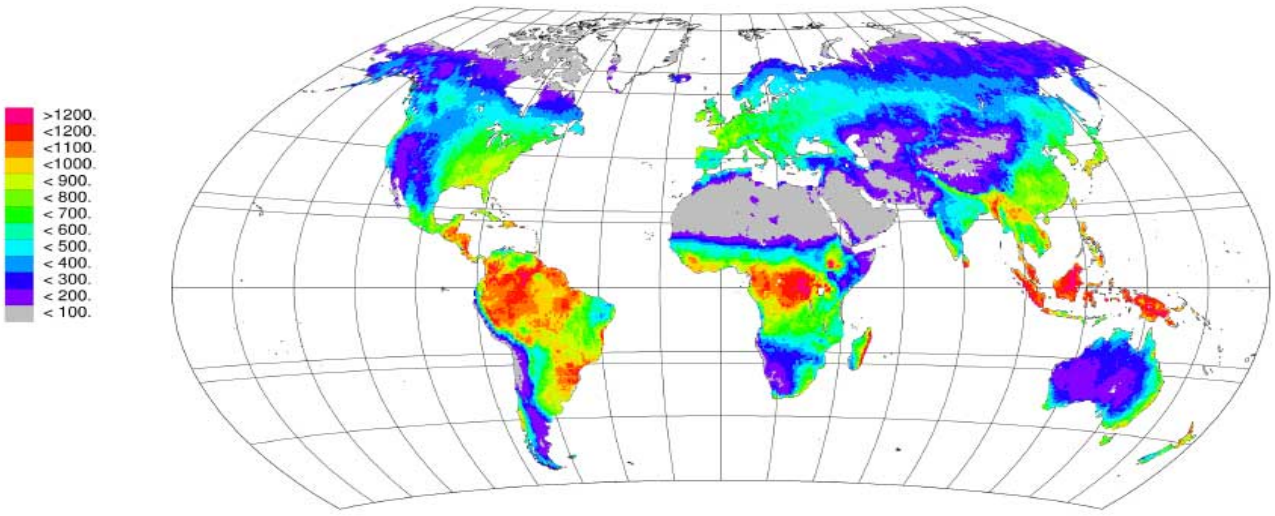

Figure 3: Annual net primary production (g C m^{-2} yr^{-1}) estimated as the average of all model NPP estimates.

(a) (b)

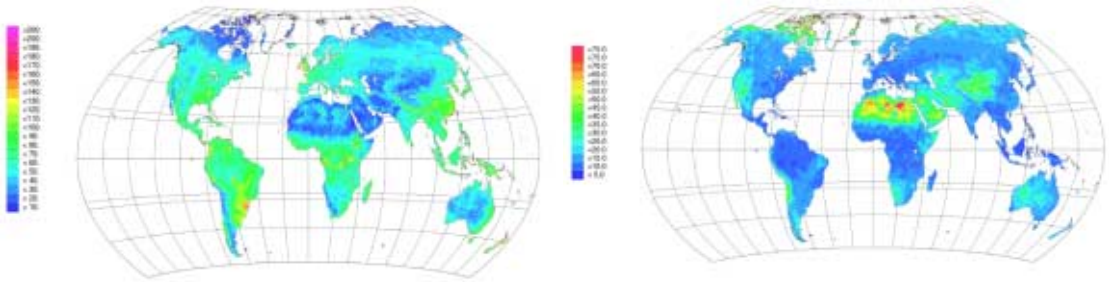

Figure 4: Spatial distribution of the variability in NPP estimates among the models as represented by (a) the standard deviation of model NPP estimated in a grid cell; and (b) the coefficient of variance of model NPP estimated in a grid cell. The coefficient of variance is determined by dividing the standard deviation by the mean of the model NPP estimates within a grid cell.

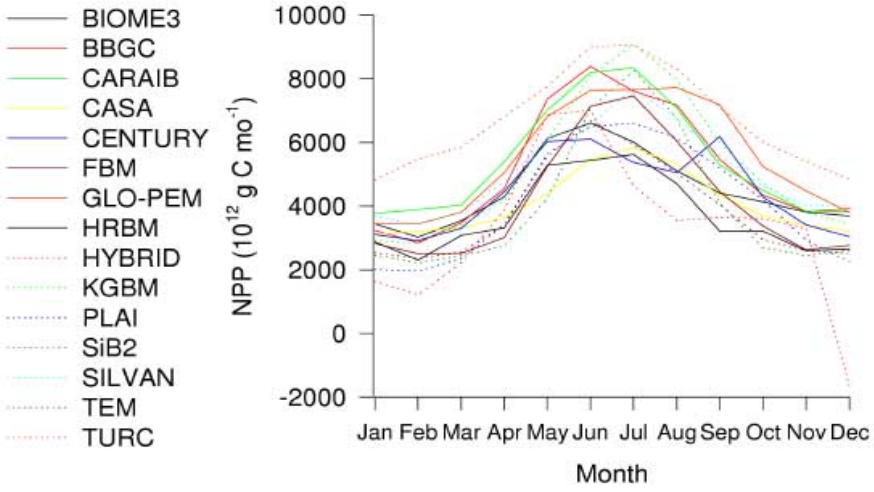

Figure 5: Comparison of seasonal variations in global net primary production among models.

varied among the models. Most models predicted the lowest NPP in February (CARAIB, CASA, TURC in January, HYBRID in December). The lowest monthly global NPP ranged from -1.6 Pg C mo^{-1} (HYBRID) to 4.8 Pg C mo^{-1} (TURC), the extremes being the same, partly for the same reasons as for the global values. A negative NPP indicates that plant respiration is greater than the uptake of carbon by plants during a month when vegetation is stressed by drought conditions or low temperatures. All models estimated that the highest monthly global NPP occurs during the northern summer, apart from CENTURY, which estimated the peak to occur in September due to a particular artifact (W. Parton, pers. comm.). The highest monthly global NPP ranged from 5.6 Pg C mo^{-1} (HRBM) to 9.1 Pg C mo^{-1} (KGBM and TURC).

The seasonal range in monthly estimates of global NPP differed among models (Table 5). The seasonal variations of HYBRID in global NPP (8.6 Pg C mo^{-1}) were more than three times larger than the seasonal variations of CASA (2.7 Pg C mo^{-1}). Table 5 shows that the intensity of the growing season was stronger in the daily models than in the monthlymodels. Models that used vapor pressure deficit (VPD) or soil moisture (SW) also estimated higher seasonal ranges in global NPP than approaches that used monthly precipitation (Prec), AET or PET. Many of the 'daily' models used variations of the Penman-Monteith algorithm to describe the influence of moisture on NPP. It appears as if the use of different algorithms to describe the effect of moisture on NPP by the various models affected the amplitude of the seasonal variations.

Comparison of the latitudinal distribution of annual NPP among models

Areally-weighted latitudinal distributions of annual and seasonal NPP estimates for fourteen key biomes were compared among the models. A trimodal distribution of annual NPP across latitudinal zones emerged with the highest areal NPP occurring near the equator (5° S to 5° N); a second, smaller peak between 35° and 45° S; and a third, smaller peak between 50° and 60° N (Fig. 6).

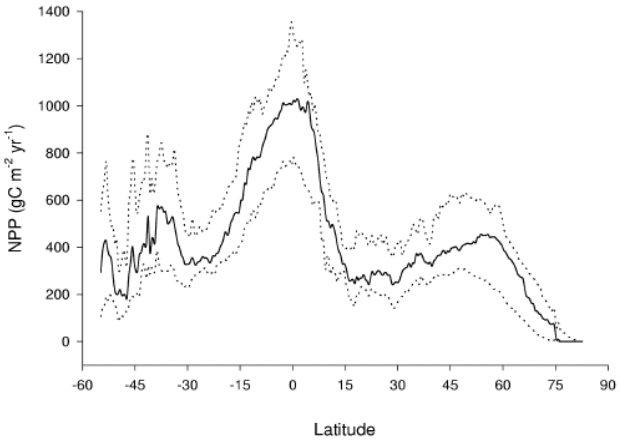

Figure 6: Comparison of the latitudinal distribution of the median (solid line), and 10th and 90th percentiles (dotted lines) of areally-weighted mean annual net primary productivity estimated by fifteen models within a 0.5^{o} latitudinal band.

There was considerable variability in the magnitude of annual NPP among all the models, particularly around the three zonal peaks; however, none of the models produced consistently higher or lower NPP across the entire latitudinal gradient. The latitudinal pattern of simulated annual NPP reflected the relative distribution and productivity of vegetation types, or biomes with NPP generally increasing from dry and cold biomes (desert, tundra) to warm, moist biomes (temperate and tropical forests) (Fig. 7). Mean annual NPP in tropical savannas was the most variable among the models, with SIB2 ranking them the second most productive. In contrast, GLO-PEM ranked tropical savannas as the tenth most productive biome of the fourteen biomes identified in the comparison of spatial variability for annual NPP.

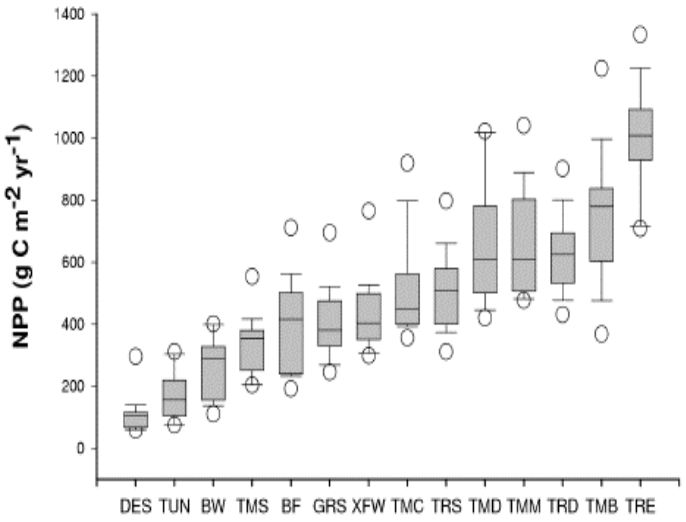

Figure 7: Box plots comparing the variability in model estimates among biomes for mean net primary productivity. Biomes included arid shrublands/deserts (DES), tundra (TUN), boreal woodlands (BW), temperate savannas (TMS), boreal forests (BF), grasslands (GRS), xeromorphic woodlands (XFW), temperate coniferous forests (TMC), tropical savannas (TRS), temperate deciduous forests (TMD), temperate mixed forests (TMM), tropical deciduous forests (TRD), temperate broad-leaved evergreen forests (TMB), and tropical evergreen forests (TRE). Biomes are arranged in ascending order of the mean biome NPP estimated from the combined model results. Bars within the boxes represent median values. The bottom and top of the box represents the 25th and 75th percentile, respectively. The bars outside the box represent the 10th and 90th percentiles. Open circles represent outliers

Comparison of seasonal NPP among models and selected biomes

Net primary productivity varied seasonally across all latitudes (Fig. 8) for all models. Over half of the models (BIOME3, BIOME-BGC, CARAIB, FBM, HYBRID, PLAI, SIB2, SILVAN, TEM) estimated a negative NPP for some latitudinal bands during some part of the year. A negative NPP indicates that plant respiration is greater than the uptake of carbon by plants during a given month. For most models, the seasonal changes of NPP were greater in the northern temperate and boreal regions than in tropical regions such that all models estimated increased NPP in northern temperate and boreal regions during some part of the Northern Hemisphere summer. However, most models also simulated a longer growing season in tropical and subtropical regions relative to northern latitudes such that annual NPP estimates were higher in these regions.

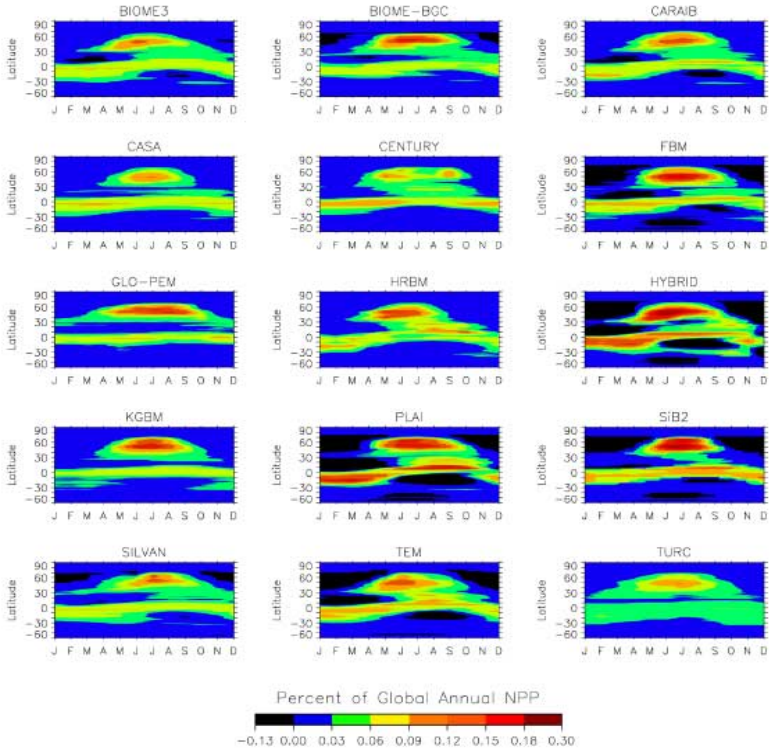

Figure 8: Relative distribution (%) of global annual net primary productivity across latitudes and months.

Comparable annual global NPP estimates did not necessarily translate into similar patterns at finer spatial and temporal resolutions among the models. For example, the CASA and PLAI models estimated a similar global NPP of about 49 Pg C yr^{1} (see above), but global NPP was distributed very differently over space and time between the two models (Fig. 8).

Additionally, large seasonal fluctuations in NPP were estimated by PLAI such that intense productivity (up to 20% of annual global NPP in a single month) occurred in a 0.5° latitudinal band during the growing season. This intense productivity compensated for large respiratory losses of carbon (up to 11% of annual global NPP in single month) during dormant periods. In contrast, CASA estimated a smaller range in seasonal NPP (between 0 and 13% of annual global NPP) such that annual global NPP was distributed more evenly over space and time.

The northern temperate/boreal latitudinal band (i.e., 50° N to 60° N) was predominantly boreal forest (51%) whereas the tropical latitudinal band (i.e., 5° S to 5° N) was primarily tropical evergreen forests (78%). Therefore, the observed variations in annual and seasonal NPP at these latitudes were likely a result of differences in model NPP formulations in these biomes. The southern temperate latitudinal band (35° to 45° S) was not dominated by any single biome and contributed a very small proportion of annual global NPP (Fig. 8). Therefore, seasonal NPP in northern boreal and tropical evergreen forests is discussed below.

Seasonal Estimates of NPP in Boreal Forests

As indicated by the seasonal patterns of the northern temperate/boreal latitudinal band (Fig. 8), NPP in boreal forests was high from June to August and low from November to March for all models (Fig. 9a). The largest differences occurred during summer (114.9 g C m^{-2} mo^{-1} in August) when all models estimated high NPP. The model estimates were most similar during the winter months (within 20.1 g C m^{-2} mo^{-1} in January) when primary productivity is low or nonexistent. These differences were due to variations in both the timing and magnitude of NPP estimated by the models.

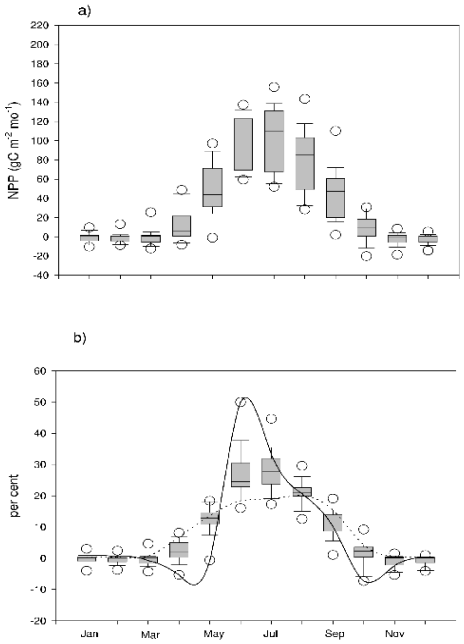

Figure 9: Box plots comparing the seasonal patterns of model estimates in boreal forests for (a) monthly NPP estimates and (b) proportional seasonal distribution of annual NPP. Bars within the boxes represent the 25th and 75th percentile, respectively. The bars outside the box represent the 10th and 90th percentiles. Open circles represent outliers. The relative seasonal distribution of annual NPP estimated by TEM (solid line) and GLO-PEM (dotted line) are presented to highlight differences in the width and breadth of the summer NPP peak estimated by all models.

Most models estimated the highest NPP in July, which was the month with the highest temperatures and precipitation at these latitudes. However, CENTURY, HYBRID, PLAI and TEM estimated the highest NPP in June, which was the month with the highest inputs of solar radiation. The models also differed on the relative size and breadth of the summer NPP peak. For example, TEM assumed a relatively narrow, but large peak of NPP with almost half of the annual NPP occurring in June (Fig. 9b). In contrast, GLO-PEM assumed a wide, but lower peak of NPP with about 20 percent of annual NPP occurring in each month from June to August. As a result of these differences, the relative seasonal distribution of annual NPP varied the most among the models in June and July. In August, the variations in NPP estimates were due mainly to differences in the assumed magnitude of NPP in boreal forests because the relative proportion of annual NPP was similar (about 20 percent) among the models.

Seasonal NPP in Tropical Evergreen Forests.

In contrast to the seasonal patterns of NPP within the tropical latitudinal band (Fig. 8), mean biome NPP simulated by most models for tropical evergreen forests was fairly constant over the year (Fig. 10a). Most of this discrepancy can be accounted for by an examination of seasonal NPP for tropical evergreen forests in the Northern Hemisphere separately from those in the Southern Hemisphere. Net primary productivity in northern tropical evergreen forests was relatively high from June to October and relatively low from December to April (Fig. 10b). In contrast, NPP was relatively high from December to May and relatively low from July to September in southern tropical evergreen forests (Fig. 10c). Thus, the different seasonal patterns of NPP in tropical evergreen forests in the northern and southern hemispheres compensated for each other when examining seasonal patterns of NPP at the global biome scale.

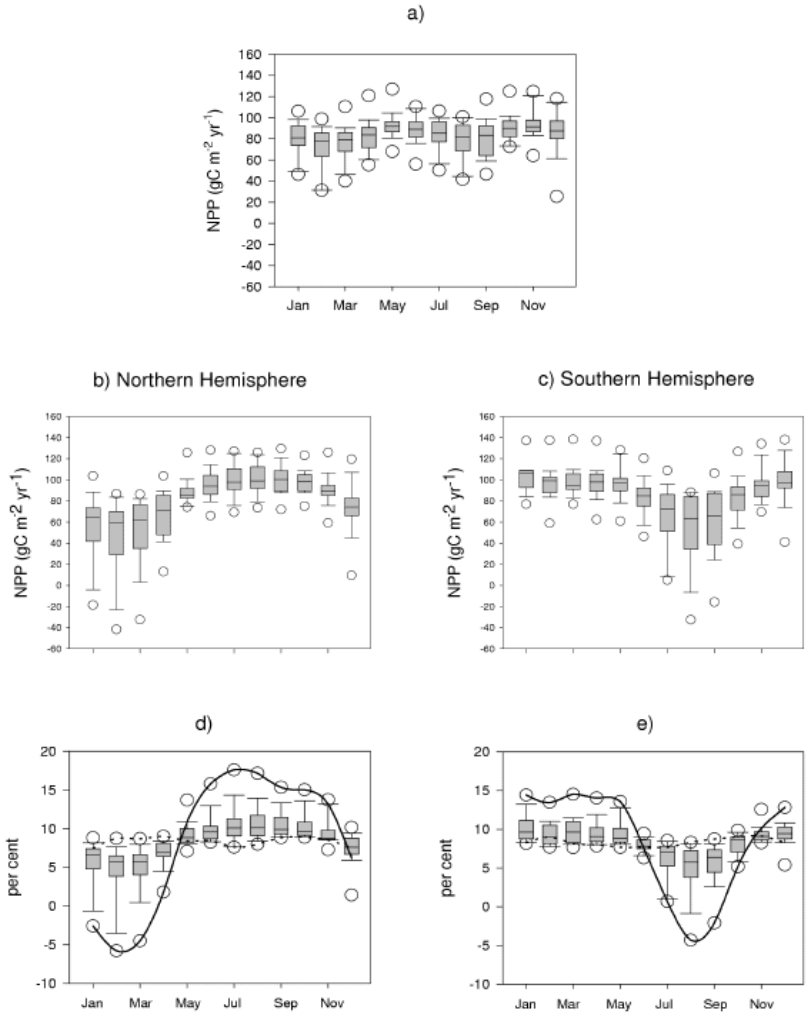

Figure 10: Box plots comparing the seasonal patterns of mean monthly NPP model estimates for (a) all tropical evergreen forests; (b) tropical evergreen forests in the Northern Hemisphere; (c) tropical evergreen forests in the Southern Hemisphere; relative seasonal distribution of annual NPP in (d) tropical evergreen forests of the Northern Hemisphere; and (e) tropical evergreen forests of the Southern Hemisphere. Bars within the boxes represent median values. The bottom and top of the box represents the 25th and 75th percentile, respectively. The bars outside the box represent the 10th and 90th percentiles. Open circles represent outliers. The relative seasonal distribution of annual NPP estimated by PLAI (solid line) and TURC (dotted line) are presented to highlight differences in relative seasonal variations of NPP assumed by the models.

Monthly NPP estimates among the models also diverged between wet and dry seasons in tropical evergreen forests of the northern and southern hemispheres. The largest range of differences occurred during the dry season in both hemispheres (up to 128.4 g C m^{-2} mo^{-1} in February for northern forests and 122.1 g C m^{-2} mo^{-1} in September for southern forests) when NPP estimates were relatively low. The model estimates were the most similar during the wet season when NPP estimates were relatively high. These differences were due to variations in both the timing and magnitude of NPP estimated by the models. For example, TURC simulated a very weak seasonality of NPP in tropical evergreen forests in the northern and southern hemisphere such that annual NPP was divided approximately equally across all months (Figs. 10d and 10e). In contrast, PLAI estimated much stronger seasonal variation in NPP in northern and southern forests such that NPP during the wet season compensated for the loss of carbon due to respiration (up to 6 percent of annual NPP per month) during the dry season.

Implications of model formulation and input datasets

Several approaches were used by the models to account for spatial and temporal variations in NPP. Each approach was based on simplifying assumptions about how ecosystems are structured and how vegetation may respond to changes in various environmental factors. As each approach is imperfect, NPP estimates were biased by the formulations and/or parameter values used by the models to develop them. For example, the formulations used in the models that calculate NPP directly (HRBM, CASA, CENTURY) never estimated a negative NPP. In contrast, the models that calculated NPP as the difference between gross primary productivity (GPP) and autotrophic respiration (R_A) could calculate a negative NPP in months when R_A was larger than GPP. As the FPAR formulations in CASA and TURC depended on the input of seasonal FASIR-NDVI data, the relatively constant monthly NPP estimated by these models in the tropics was partly explained by the weak seasonality of the remotely sensed data set. The weak seasonality of the NDVI data in the tropics suggests that the seasonal drought conditions may not be as pronounced as indicated by most of the NPP models. This may be partly explained by Nepstad *et al.* (1994) who observed that tropical trees can have roots down to soil depths greater than 8 meters such that evergreen forests may be able to maintain evapotranspiration during five-month dry periods by accessing deep soil water. Most of the NPP models in this intercomparison had rooting zones for tropical forests that ranged from 1 to 3 m. Therefore, the simulated vegetation would never have access to deep water resulting in decreased NPP and a more pronounced

seasonality relative to those models driven remotely sensed phenology. The use of NDVI by the CASA and TURC models may have implicitly accounted for the effects of deep rooting on phenology, but other models that use NDVI data (e.g. GLO-PEM, SIB2) still simulated a pronounced seasonality in the tropics, suggesting that some other phenological or ecophysiological mechanism was driving NPP cycles in these models.

Seasonal variation in global net primary production across environmental gradients

Solar radiation is a driving variable for photosynthesis and precipitation, temperature and nutrients are major constraints [*Lieth*, 1975]. During the course of a year, vegetation may respond to variable climate by shedding tissue. Alternatively, the living biomass can avoid activity during cold or dry periods. Most current global models of NPP simulate biogeochemical fluxes at monthly or shorter time steps in the course of an average year, and therefore, explicitly acknowledge the variability of resource availability over time. In addition, these models also account for the seasonal changes in photosynthetic capacity as leaves grow and senesce throughout the year. Models which simulate phenology and canopy development consider different hypotheses for the seasonal profile of the leaf area index (LAI) depending on the plant functional types (PFT) within the various biomes. Seasonal changes, such as the development and shedding of foliage, or dormancy strategies due to cold or dry conditions, are easily observed in most ecosystems and are therefore features of most physiognomic classifications of vegetation. A comparison between the simulated timing and amplitude of seasonal changes in biospheric fluxes to observed (e.g. satellite data) yields an indication of model performance.

To analyze simulated phenology, two main categories of global NPP models were considered: 1) models driven by satellite data to estimate the temporal variations of the fraction of absorbed photosynthetically active radiation (FPAR); and 2) models that simulated the temporal behavior of the canopy (i.e., changes in LAI) using climate and soils data alone. Thus, the

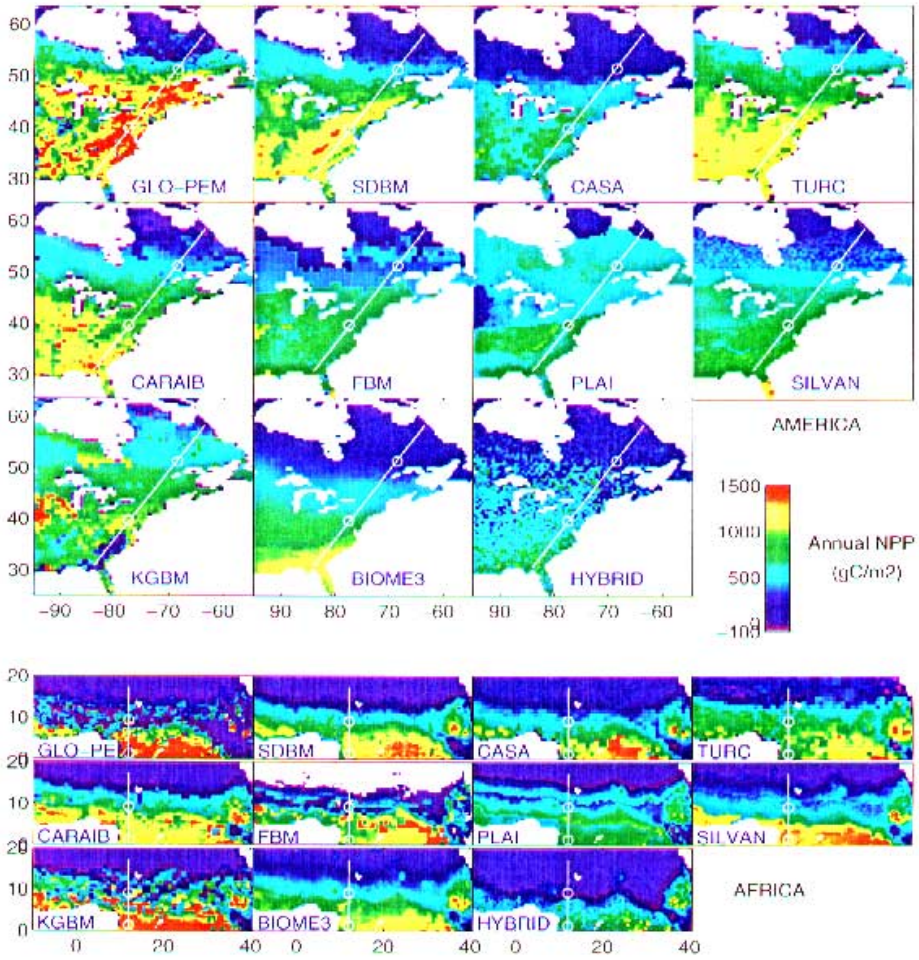

Figure 11: Annual NPP over eastern North America (top) and central Africa (bottom) estimated by 11 NPP models. The position of the transect and the location of the individual grid cells are marked in each case. The PEMs are grouped on the first row. The canopy models simulating both phenological development and biogeochemical fluxes according to some vegetation map are grouped on the second row. KGBM and models of vegetation structure and function are grouped on the third row.

importance of the radiative activity of the canopy was explicitly recognized (either derived from satellite observations or simulated) for carbon assimilation. The seasonal absorption of the photosynthetically active radiation, as well as the relationships between absorbed radiation and photosynthesis were examined to explore the differences among predicted NPP. By converting LAI to FPAR, the importance of the description of leaf phenology for the estimation of the seasonal NPP fluxes could be evaluated.

To determine whether differences in the seasonality of NPP among models were explained by either the canopy radiative behavior forcing the seasonal radiation or by differences in the seasonal conversion of the absorbed PAR (APAR) into carbon, also referred to here as light-use efficiency (LUE), the environmental constraints affecting the relationship of FPAR and LUE to NPP were examined over regions with a strong gradient of the major driving climatic variables responsible for the seasonal cycle. Summergreen phenology was analyzed along a temperature/radiation gradient in North America, and raingreen phenology was analyzed along a precipitation gradient in Africa (Fig. 11). Because many models used a prescribed vegetation distribution (or simulated the vegetation distribution together with the NPP), it was useful to look at the changes in simulated seasonal NPP behavior at ecotones, for example, the transition from evergreen to deciduous forests.

To simulate phenology, canopy models generally used one of two different strategies: 1) a separate module estimated the timing of crucial phenological events such as leaf on/off dates, without considering the current NPP values, or 2) phenological stages were directly determined from the current carbon balance, i.e. NPP. The same model may have utilized both strategies, depending on the vegetation type (Table 6).

Table 6: Strategies used by the canopy models to simulate phenological development and to determine the LAI. For more detailed explanation (parameterization of the separate phenological module, limitation of LAI growth for models considering allocation to leaves), see text.

	Phenological module		LAI estimates	
	unrelated to NPP estimates	related to NPP estimates	no specific allocation relationship of assimilated carbon to leaves	carbon allocation to leaves using SLA
CARAIB	N/A*	all ecosystems	Optimization of the monthly LAI on the basis of a monthly carbon balance	N/A
FBM/PLAI	N/A	all ecosystems	N/A	daily conversion of the green biomass to leaves
SILVAN	temperate deciduous	water dependent	N/A	6 days conversion of the assimilate pool to leaves
KGBM	all deciduous	N/A	Optimization of the maximal yearly sustainable LAI on the basis of the water resources	N/A
BIOME3	all deciduous	N/A	maximum yearly sustainable LAI which optimizes NPP on the basis of the water resources & satisfies the whole plant-carbon allocation requirements	N/A
HYBRID	cold + dry deciduous trees	grass	N/A	daily allocation to leaves for grass yearly allocation to leaves for trees

* N/A: Not Applicable

To examine whether the differences in annual estimates of global NPP were related to general differences in the growing season as it was estimated by the models, seasonal estimates of global NPP were compared among the models across environmental gradients for eastern North America and Africa (Fig. 12). Most of the models predicted increased NPP southward with annual temperature and radiation increases in America or with increased annual precipitation in Africa. However, annual NPP sometimes differed up to 200% between models. All models except KGBM predicted similar NPP values for the non-vegetated Sahara and the tundra, but differed by over 100% in the more productive areas.

Evaluation of the simulated seasonal FPAR against FASIR-FPAR

The NDVI-derived FPAR from the PEMs was strongly correlated to monthly FASIR-FPAR (Table 7) for global and the four biome-types analyzed, whereas correlations were weaker from canopy models. Generally, the simulated seasonal FPAR agreed well with the FASIR-FPAR for the temperate deciduous forests, and the highest correlations occurred with SILVAN, which calibrated its phenology submodel for temperate and boreal biomes using satellite observations. These relatively high correlations were obtained despite the fact that a large part of the natural area for deciduous forests was under cultivation, where the timing of harvest removal strongly influences the satellite FPAR. In North America, however, crops are primarily spring/summergreen, roughly in phase with temperate deciduous forests. There were fairly weak correlations between simulated and satellite-derived FPAR for savannas, and boreal forests.

Table 7: Monthly grid cell level correlations ($P < 0.1$) between the modeled FPAR and the satellite FASIR-FPAR for the globe and four major ecosystems. The first three models are PEMs, the remainder are canopy models. GLO-PEM is not considered because this model used the FASIR-FPAR directly.

	global	boreal forest	temperate deciduous forest	savanna	evergreen tropical forest
SDBM	0.884	0.873	0.919	0.822	0.836
CASA	0.994	0.997	0.996	0.991	0.993
TURC	0.946	0.962	0.975	0.937	0.94
CARAIB	0.736	0.683	0.613	0.711	0.301
FBM	0.6	0.351	0.728	0.498	0.173
PLAI	0.593	0.496	0.788	0.46	0.11
SILVAN	0.682	0.642	0.878	0.507	0.518
KGBM	0.563	0.420	0.742	0.559	0.154
BIOME3	0.657	0.468	0.388	0.584	0.188
HYBRID	0.696	0.351	0.728	0.498	0.173

The poorest correlations were from tropical evergreen biomes where seasonal changes in the canopy cover were limited. While both simulated FPAR and FASIR-FPAR were relatively constant throughout the year, a positive correlation simply indicated that the spatial variability of FPAR values were in agreement, however, at times, their absolute values still strongly disagreed. These results suggest that the models better represented the seasonal effects of the variability in solar radiation and temperature on canopy development for summergreen deciduous forests relative to the effects of the seasonal precipitation on canopy development in the raingreen savanna.

Seasonality of FPAR, LAI and NPP along the American gradient

The phase diagrams of seasonal FPAR along the transect (Fig. 12) reflect the spatial/temporal results of the correlations described above for boreal forests and temperate deciduous forests. In general, the seasonal changes in FPAR estimated by the PEMs across the transect represent the seasonal changes in FASIR-FPAR (i.e. the FPAR for GLO-PEM) better than the corresponding FPARs of the canopy models. Although the seasonal pattern of simulated FPAR for many of the canopy models may be similar to the FASIR-FPAR, the magnitude of the simulated FPAR was often much higher. In both PEMs and canopy models, the FPAR associated with boreal forests and broad-leaved evergreen mixed forests in the transect varied less over the year than the FPAR associated with other vegetation types. However, the models often did not agree on the distribution of vegetation along the transect.

The seasonal patterns in FPAR were similar across the transect for the PEMs using the FASIR-NDVI (CASA, GLO-PEM and TURC). The highest FPAR calculated by these models occurred during the summer months. In boreal forests, TURC was not calibrated the FASIR-NDVI dataset, resulting in an overestimation of FPAR in boreal forests. The seasonal pattern of FPAR estimated by SDBM had the greatest divergence from the FASIR-FPAR in this transect. Note that there were no sharp transitions in the seasonal patterns from SDBM at the ecotones bordering boreal forests as were found in the seasonal pattern of the other PEMs using the FASIR data. Unlike the FASIR interpolation [*Sellers et al.*, 1994] for the boreal forest, no such vegetation-dependent processing was applied in the Gallo-NDVI data set used by SDBM.

Typically, the FPAR simulated by the canopy models predicted discontinuities at the ecotones. Several canopy models predicted a later FPAR increase in the spring and summer and a later decrease in autumn and winter than was indicated by the satellite-derived FPAR data. The seasonal features of simulated FPAR were directly related to the seasonal estimates of LAI by the canopy models; i.e. quasi-constant LAI for evergreen ecosystems, no active vegetation (LAI = 0) in winter for the temperate deciduous ecosystems. The range of estimated LAI values among the models was large (e.g., between 1 and 10 for the taiga), and appeared too high in several cases. Chen (1996) reported that the LAI of most boreal conifers are less than 3, and only aspen/hazel stands tend to have LAI values exceeding 5. There are several plausible reasons why canopy models simulated high LAI values. For example, the annual LAI of KGBM was constrained only by water availability and not by carbon or nitrogen limitation. High LAI predictions highlight the differences between the FPAR calculated from the canopy models and the FPAR estimated from the PEMs in the boreal forests.

Stronger correlations between seasonal FPAR the PEMs within deciduous forests were related to: 1) similarities in simulated phenology for the canopy models and observed phenology for the PEMs, and 2) the more realistic maximum LAI (i.e. LAI ranges from 4 to 8) estimated by the canopy models. Temperate broadleaf deciduous forests in eastern North America rarely exceed an LAI of 6. In contrast, the models disagreed on the timing of maximum LAI in deciduous ecosystems, e.g. the maximum LAI of deciduous forests occurred later in FBM and PLAI than the other models.

Along the American transect, the seasonality of NPP reflected, to some extent, the seasonality of FPAR (Fig. 12). For ecosystems dominated by deciduous trees, the differences in the phase of the seasonal NPP among models along the transect were largely determined by the seasonal FPAR features of each model, highlighting the importance of the temporal profile of the canopy structure for determining seasonal NPP. However, high monthly estimates of FPAR did not always correspond

with high monthly estimates of NPP (e.g., boreal forests). Thus, factors other than FPAR likely influenced the seasonal NPP estimated by these models.

Seasonality of FPAR, LAI and NPP along the African gradient

Similar to the results of the American transect, the seasonal changes in FPAR estimated by the PEMs across the African transect (Fig. 13) represented the seasonal changes in FASIR-FPAR (i.e. the FPAR for GLO-PEM) better than the corresponding FPAR's from the canopy models. Again, the magnitude of the simulated FPAR of the canopy models could be much higher than the FASIR-FPAR, particularly in the southern part of the transect, but only the seasonal pattern of simulated FPAR for CARAIB, SILVAN and KGBM reflected the seasonal pattern of the FASIR-FPAR across the transect.

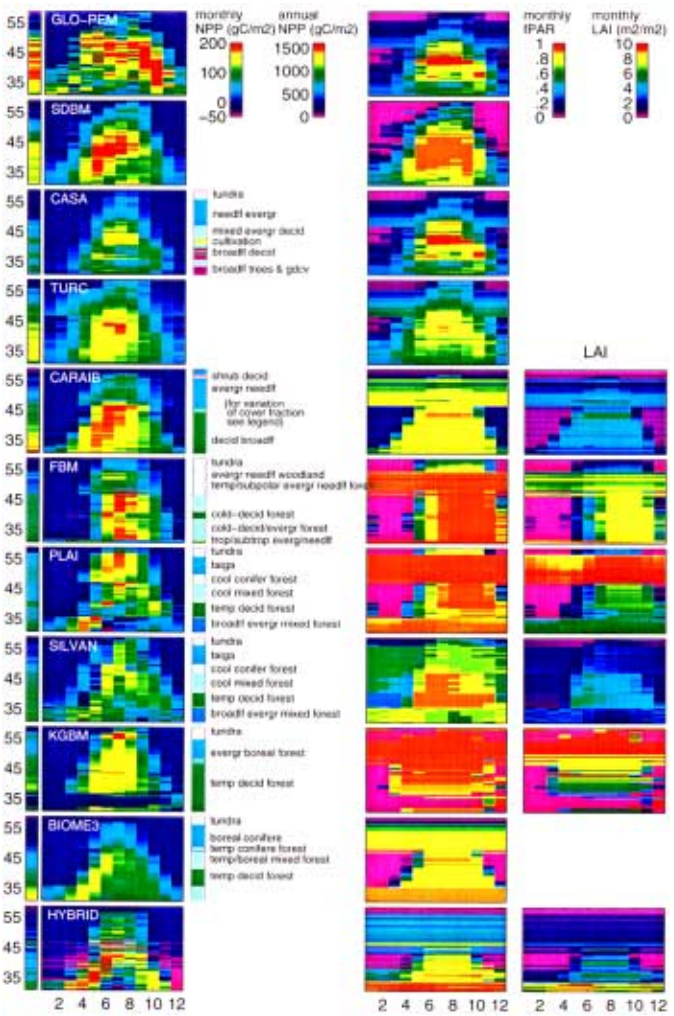

Figure 12: Phase diagrams of the monthly NPP, FPAR and LAI (only for the canopy models) along the north-south transect (radiation and temperature gradient) over eastern North America: (58.5 °N, 63.5 °W) to (31 °N, 84 °W). The order of the models is the same as before. The horizontal axis denotes the 12 months, the vertical the latitudes. For each model, the annual NPP along that transect is indicated on the left side of the phase diagram of monthly NPP, and an indication of the vegetation structure associated with each grid cell, is indicated on the right side when the model employs one, either as input, or as output (BIOME3). For CARAIB, only the forest type is indicated, but the model works with cover fraction of different PFTs within each grid cell: forest cover fraction increases regularly from the north to the boundary between evergreen and deciduous (from 10% to 80%), while C_3 grass cover fraction decreases in the same direction (from 50% to 20%). Then deciduous broadleaf forests and C_3 plants (grasses + crops) share the southern part.

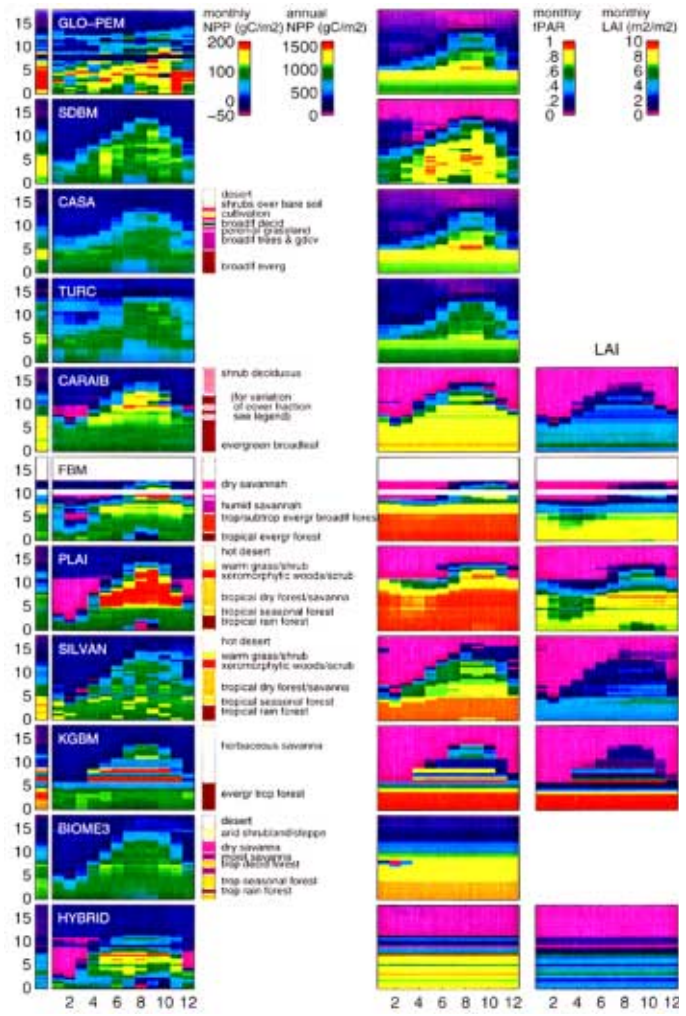

Figure 13: The same as Fig. 11 for the north-south transect (precipitation gradient) in Africa (17.5 ˚N 12 ˚E to (0 ˚N 12 ˚E. For CARAIB, the southern end of the transect has a maximum forest cover fraction (80-100%), the middle part has C_3 grasses and crops (around 40%), C_4 grasses and crops (around 20%) and forest (around 10%), and the northern part only a 10% cover of C_4 grasses.

In both the PEMs and canopy models, the FPAR associated with tropical evergreen forest transect varied less over the year than the FPAR associated with other vegetation types. For the PEMs using the FASIR-NDVI, this seasonal pattern was the result of the reconstruction to a constant value throughout the year [*Sellers et al.*, 1994]. For the canopy models, the simulated FPARs again reflected LAI estimates. Model estimates of LAI for the tropical evergreen forest grid cells of this transect varied between 3 and 12, whereas field studies have indicated that LAI can reach values of 8 or 10 for African evergreen rain forests [*Walter and Breckle*, 1983]. Although most canopy models did not estimate such high LAIs, the corresponding FPARs of these models were generally higher than the FASIR-FPAR. The low values of the FASIR-FPAR in the southern part of the transect may reflect the influence of constant cloud contamination on the NDVI signal. This raises questions about the validity of using optical satellite data to represent changes in the vegetation canopy in tropical forests.
As was shown for the American transect, the models often did not agree on the assumed distribution of vegetation used to develop NPP, LAI and FPAR predictions across the African transect. There were strong disagreements among the models on the northern limit of evergreen canopy, some models clearly assumed evergreen vegetation where the NDVI derived FPAR data indicated deciduous vegetation. Some of these discrepancies resulted from the fact that some models assumed savannas as a grassland, whereas other models simulated a mixture of trees and grasses.

The seasonality of NPP reflected, to some extent, the seasonality of FPAR over the African transect for most models (Fig. 13). However, high monthly FPAR predictions rarely corresponded with high monthly estimates of NPP. Thus, as with North American forests, factors other than FPAR likely influenced the seasonal NPP estimates of the models in this transect. Differences in FPAR among the models may be compensated for by associated differences in LUE. For example, the simulation of a green canopy in the savanna when the conditions were not favorable (e.g., dry season; Fig. 12) may have resulted in negative NPP predictions from some models (FBM, PLAI, HYBRID) because of respiration costs. As a result, seasonal NPP patterns were similar to those estimated by other models that predicted positive NPP, even though the seasonal patterns of FPAR and the absolute monthly NPP values were very different. For some calibrated models, respiration losses have to be compensated for by high monthly productivity during the active period (200-250 g C m^{-2} for PLAI and FBM and somewhat less for CARAIB). Therefore, these models estimated productivity rates during the active months which were close to the efficiency of crops growing under optimal conditions (i.e. 1 g C MJ^{-1} APAR). Le Roux *et al.* (1997) found a production efficiency of only 0.86 g C MJ^{-1} APAR during the growing phase and 0.58 g C MJ^{1} APAR at maturity in productive humid savannas.

The similar correlations between NPP and APAR as well as NPP and LUE among the models in boreal evergreen and temperate deciduous forests imply a general consensus on the effects of radiation in ecosystems with summergreen phenology. Correlations among the seasonal changes in solar radiation, temperature and FPAR in these ecosystems suggest that the influence of seasonal changes in canopy on NPP may be partially accounted for in models that only considered the influence of climate variables on NPP. In contrast, the different correlations of NPP with APAR and LUE among the models in savannas and tropical evergreen forests suggest little agreement on the influence of the canopy on simulated NPP in ecosystems with raingreen phenology. Additional studies that collect seasonal soil moisture data concurrently with seasonal LAI and FPAR data in these ecosystems would allow a better evaluation of the relationships among these variables and improve our understanding of raingreen phenology.

Importance of vegetation distribution and parameterization on FPAR, LAI and NPP
Models that assumed homogeneous vegetation characteristics within biomes usually considered only one set of parameters for each biome. This parameterisation included the decision to assign a vegetation type as evergreen, deciduous or mixed in its canopy seasonality. As a consequence the models generally exhibited sudden changes of various simulated variables (e.g., FPAR, NPP see Figs. 11,12, and 13) at ecotones where the value of some parameters might suddenly change. This was particularly true for the canopy models but also for all the PEMs that used the FASIR data due to their vegetation-map related processing. Along the two transects, differences in the vegetation maps and associated parameters among the models influenced seasonal LAI, FPAR and NPP among the models at least as much as the differences in model assumptions about ecophysiology. Often, these differences in seasonal NPP across ecotones were manifested as banding patterns (e.g., FBM, PLAI, SILVAN and BIOME3) or small scale spatial variability (e.g., GLO-PEM, SDBM, CASA, TURC, CARAIB, KGBM, HYBRID) for annual NPP (Fig. 11). Differences in the spatial pattern of vegetation structure among the models may have been caused by: (1) the better spatial resolution of vegetation characteristics by NDVI data (e.g., SDBM, CASA, TURC, GLO-PEM, KGBM); (2) the representation of ecosystems as a mosaic of plant functional types (e.g., CARAIB) rather than a dominant vegetation type; and (3) stochastic initialization of the biogeography component of dynamic vegetation models (e.g., the gap model in HYBRID).

This analysis suggests that APAR and LUE may not be totally independent. In evergreen ecosystems where high LAI generated high APAR, maintenance respiration costs during months with unfavorable conditions may have been influenced by low LUE. This relationship was more obvious in the calibrated canopy models than in the uncalibrated canopy models (BIOME3, HYBRID, KGBM). It appears as if the calibrated models used parameterisations that enforce the negative link between APAR and LUE. A negative correlation between global APAR and global LUE among the different models is noted below.

Correctly calibrated models are required to give stable NPP estimates and to aid in the evaluation of uncalibrated models, however, the accuracy and representativeness of the field data found in the ecological literature is still a matter of debate (Kohlmaier *et al.* 1997). It should also be noted that field measurements of LAI are likely to be biased toward high values, which are more representative for well developed sites chosen by ecologists rather than the average condition of vegetation contained in an average 0.5 degree grid cell.

Field measurements of NPP usually occur over a temporal resolution of a few months to a year. Therefore, other sources of information must be used to infer the validity of seasonal NPP estimates. In deciduous ecosystems, the positive correlations between simulated seasonal FPAR and FASIR-FPAR from satellite data provide some confidence in the seasonal behavior of some models, but this does not *per se* constitute a validation of seasonal NPP. Models with similar seasonal FPAR can simulate very different seasonal NPP, and vice-versa, due to different assumptions and parameterisations that determine LUE.

Although satellite data may not be useful for evaluating NPP directly, this analysis suggests that surrogate measures of vegetation structure (i.e. FPAR) are useful for evaluating seasonal changes in NPP. However, there was some variability in the phenology portrayed by the FPAR derived from different NDVI data sets and the algorithms used for the FPAR computation (cf. Figs. 11, 12, and 13). Consequently, a single satellite data set cannot be considered as a sufficiently precise evaluation tool. Furthermore, the one month's resolution of the satellite data set used here is not sufficient to determine spring growth accurately and to test the simulated timing of budburst, in which a shift of 15 days may have considerable effect on estimates of annual production.

The importance of water availability to primary productivity in global terrestrial models

Water availability is a primary factor controlling NPP. A number of studies tend to support this assumption for most of the world's upland ecosystems. Initially, Rosenzweig (1968) predicted NPP of terrestrial plant communities from actual evapotranspiration. Lieth [*Lieth*, 1975] then determined a curve describing the relationship between annual precipitation means and NPP of ecosystems unlimited by low temperatures. Later, a water balance which integrated precipitation input, soil water storage and atmospheric evaporative demand was found to be the dominant control of leaf area index and NPP in forests of the northwestern United States [*Gholz*, 1982; *Grier and Running*, 1977]. Finally, Stephenson [*Stephenson*, 1990] and Neilson *et al.* [*Neilson et al.*, 1992] illustrated strong correlations between the distribution of the North American plant formation with water-balance parameters. Thus, the results from these studies suggest that the water balance is likely a dominant factor responsible for predicting patterns in NPP. To set the stage, the definitions of actual and potential evapotranspiration (AET and PET) and their estimation methods in several global models are discussed. This approach is essential for evaluating how simulated approaches may impose water budget limitations on NPP. Next, the models' time steps were compared and the methodologies evaluated for calculating critical water balance parameters such as canopy interception and evaporation, soil moisture and snowpack treatment. Finally, the relationships between a water balance coefficient and simulated NPP from the global models were analyzed.

The assumption that water availability is the primary limiting factor of NPP was tested for the following models: BIOME-BGC, BIOME3, CARAIB, CASA, CENTURY, GLO-PEM, FBM, HRBM, KGBM, PLAI, SDBM, SILVAN, TEM and TURC. Different approaches have been evaluated and used in these models for introducing water budget limitations on NPP. Three methods to restrict NPP by water availability in global NPP models were distinguished. The first included a direct physiological control on evapotranspiration through canopy conductance. Secondly, climatological supply/demand constraints on ecosystem productivity were calculated. Finally, a water limitation was inferred from satellite data alone. In addition, a water balance coefficient (WBC) was calculated as the difference between mean annual precipitation and potential evapotranspiration and compared to NPP for each grid cell in each model. The NPP versus WBC correlation plots exhibited comparable patterns among the models using the same methods for water balance limitations on NPP. While correlation plots revealed similar boundary lines for most global models, there was considerable variability in these distributions related to numerous environmental controls on NPP. The models with physiological control on evapotranspiration had the highest variability in those distributions because they were able to capture effects of more environmental controls on NPP.

As discussed above, there were vast differences in logic employed by the different models accounting for water availability and its subsequent limitation on NPP. As a result, the direct comparison of water balances in different models was not possible, and general characteristics of the models had to be considered in order to test this assumption. To compare the estimated annual NPP in relation to water availability among global models, a water balance coefficient (WBC) reflecting water availability was defined as the difference between precipitation (Precip) and potential evapotranspiration (PET):

$$WBC = Precip - PET \qquad \text{Equation (1)}$$

The potential evapotranspiration was computed as a function of temperature and radiation from Priestley and Taylor (1972):

$$l\,PET = a\,[s/(s+g)](R+G) \qquad \text{Equation (2)}$$

where l PET is the latent heat flux density, a is Priestley-Taylor parameter, R is the net radiation above the surface, G is the soil heat flux, s is the slope of the saturation vapor pressure-temperature curve at the dry bulb temperature, g is the psychrometer constant. In this analysis, R was calculated as the proportion of net solar radiation and G was a function of temperature. Water balance coefficients calculated by the method described above had the advantage of being independent of any model results and dependent only on input climate data. The global annual water balance coefficient was calculated at

each grid cell (0.5° x 0.5° longitude/latitude) as a simple scalar that could be used with all models, regardless of their individual hydrologic computations (Fig. 14).

Assuming that water availability was the primary controlling factor of global NPP patterns, NPP limitation ranges by the WBC were scrutinized. In dry regions, gradually increasing water availability facilitates the regular increment of maximum potential vegetation productivity. If an ecosystem receives sufficient water available for vegetation, then moisture is not a limiting factor and the maximum NPP saturates. At high WBC, NPP below maximum reflects control by other climatic variables. For example, at high latitudes, low annual sunlight inhibits NPP and in cold climates low temperatures restrict photosynthesis and NPP. In addition, low nutrients may limit optimum NPP in some areas.

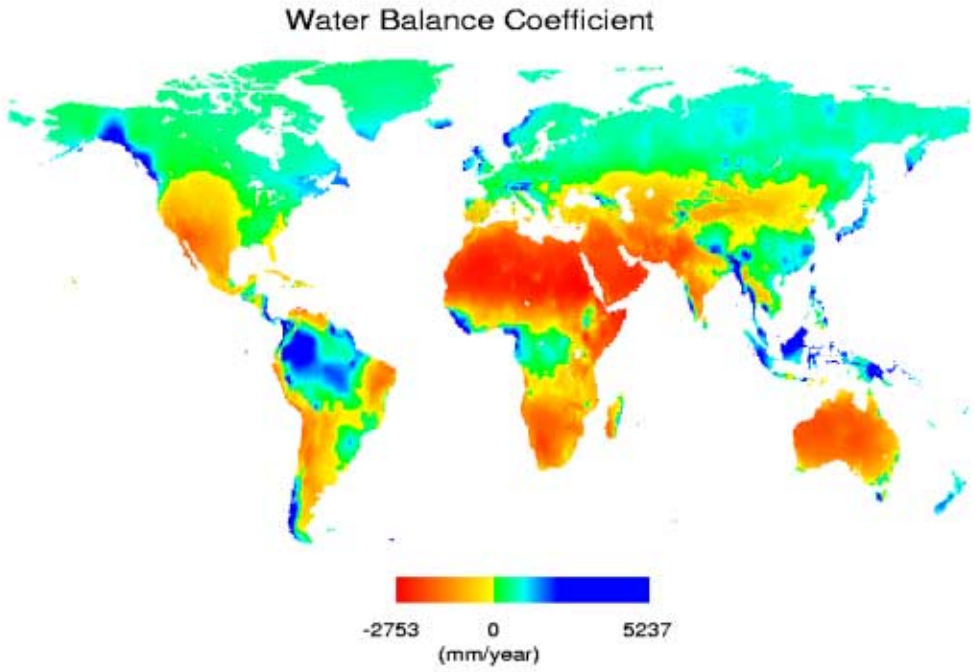

Figure 14: Water balance coefficient computed as the difference between annual precipitation and potential evapotranspiration (eq. 1). This coefficient was calculated at each 0.5° x 0.5° longitude/latitude grid cell. Potential evapotranspiration computed by Priestley-Taylor method (eq. 2) using the Cramer and Leemans (1993) global climate databases.

A comparison of NPP estimated by the various models to WBC for all the grid cells of the globe (Figs. 15, 16,17) indicated low correlation (R^2 = 0.05-0.3) between these two variables. However, a closer examination of these correlation plots revealed some general characteristics of the relationship between WBC and NPP for all models. As the WBC became increasingly more negative, the upper boundary of NPP estimates decreased in all models. The decrease of the upper boundary indicated that water was the ultimate limiting factor of NPP in these grid cells. However, the wide distribution of NPP estimates between zero and the upper boundary in this part of the correlation plots indicated that secondary factors simultaneously limit NPP at these grid cells. These secondary factors probably included differences in temperature, solar radiation, and/or nutrient constraints among models. Grid cells with a negative WBC covered a large proportion of the globe (Fig. 14). Spatial variations in the density of NPP estimates in this part of the correlation plots suggested that the interaction among the various environmental controls was different among the models. Around WBC equal to zero, there was a large density spot of grid cells with low NPP estimates (Figs. 15,16,17). These estimates represented the productivity of tundra and boreal forests where the difference between annual precipitation and evapotranspiration demand was subtle together with NPP primarily limited by low temperatures (Fig. 14). As the WBC became more positive, NPP estimates from many models appeared to reach a maximum of 1500 to 3000 g C m^{-2} y^{-1}. These estimates represented the NPP of moist tropical regions. For BIOME-3, CARAIB, FBM, KGBM, PLAI, SILVAN and TEM, the high density of NPP estimates at this maximum indicated that the models assumed optimum environmental conditions for NPP for most grid cells within this region. The other models had more variability in NPP estimates for the moist tropics indicating the importance of secondary factors such as nutrient constraints or land-use in these regions. The maximum NPP predicted by the models varied over a WBC range from -1500 to 800 mm y^{-1}, or, about one-fourth of the entire range of the WBC estimates. Half of the models (i.e., BIOME-3, CARAIB, CASA, FBM, GLO-PEM, SILVAN and TURC) estimated the maximum NPP to be in regions with a negative water balance. In contrast, BIOME-BGC, CENTURY, HRBM, KGBM, SDBM, TEM and PLAI predicted the maximum NPP to occur where the water balance was positive.

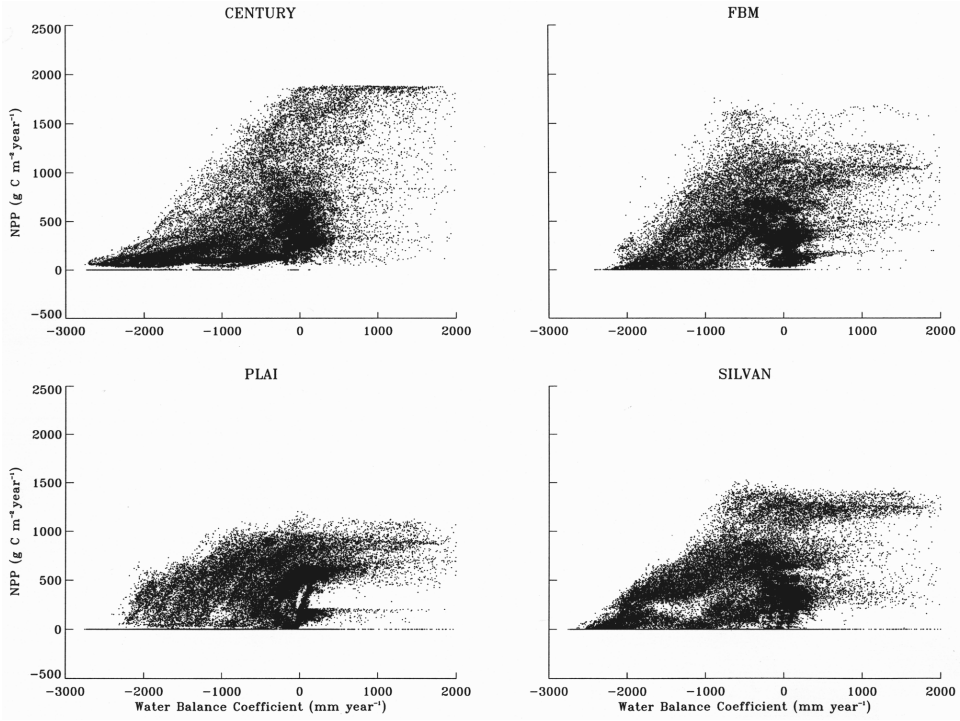

Figure 15: Relationship between estimated NPP and water balance coefficient for models with physiological control on evapotranspiration through stomatal control. Each data point represents one 0.5 ^{o} x 0.5 ^{o} longitude/latitude grid-cell.

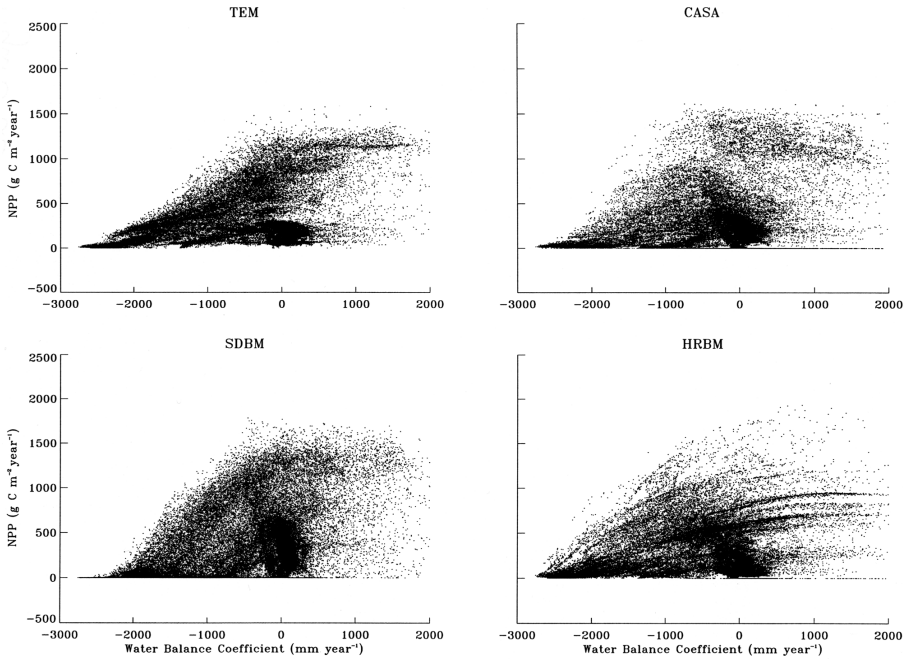

Figure 16: a, b. Relationship between estimated NPP and water balance coefficient for models with climatic supply/demand control on ecosystem productivity. Each data point represents one 0.5^{o} x 0.5^{o} longitude/latitude grid-cell.

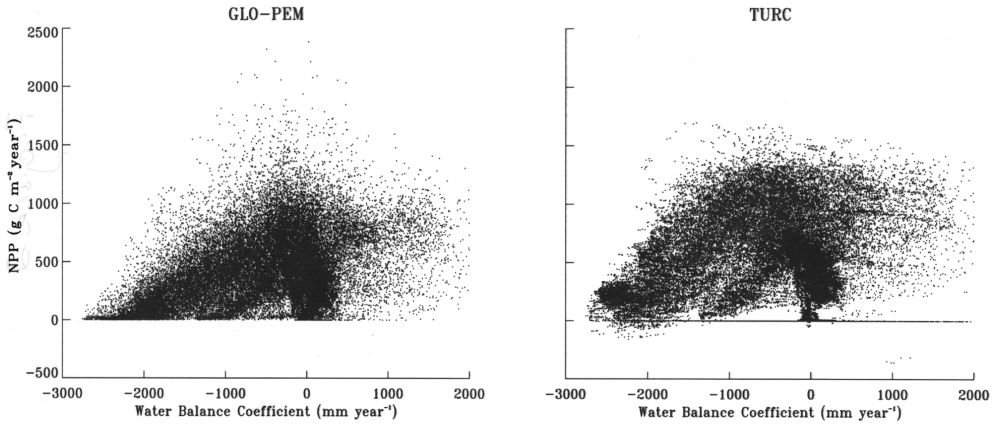

Figure 17: Relationship between estimated NPP and water balance coefficient for models with water availability limitation inferred through satellite data. Each data point represents one 0.5^{o} x 0.5^{o} longitude/latitude grid-cell.

A number of reasons can account for the differences in the model results discussed above. As the various models used different functions to calculate PET from the approach used to compute the water balance coefficient, the variations in the relationship of maximum NPP to WBC may be a result of these differences. It is also acknowledged that the WBC calculated on an annual basis does not account for seasonality of precipitation or the interaction of seasonality of precipitation and PET. Overall, it is important to mention that a WBC does not provide an absolute measure for water balance, but it supplies a general scale of the potential water increment within an ecosystem.

It appears that the methods used to estimate water budget limitation on ecosystem productivity had a significant effect on the model outputs. Models with physiological controls over evapotranspiration and NPP consequently were characterized by even distributions of NPP versus the water balance coefficient (Fig. 15). This implies that a variety of additional environmental factors may be controlling ecosystem productivity. In addition, these models predicted a smooth increase in the range of NPP with an increasing WBC and the slope of the edge of NPP versus WBC was steeper (except BIOME-3) suggesting that the deficit of water available to plants set the upper limit on ecosystem productivity.

While water balance may be the most influential control on global NPP, regional and biome specific NPP variability must be described with more than water balance alone. Improved biospheric models should account for multiple environmental factors controlling global NPP in a non-linear fashion for the most accurate solutions.

NPP, NDVI and climate space

To analyze the broad-scale behavior of fifteen global biosphere models, the sensitivity of simulated net primary productivity (NPP) to precipitation, temperature, solar radiation, and to the Normalized Difference Vegetation Index (NDVI), was evaluated spatially and temporally. Annual NPP estimates for 41,344 grid cells were averaged across all models and compared to annual precipitation and mean annual temperature of associated grid cells as well as the corresponding coefficient of variation of the average NPP estimates. To relate the latitudinal distribution of NPP to climate and NDVI, the areally-weighted mean annual precipitation, temperature, solar radiation and NDVI (1987 FASIR-NDVI, [*Sellers et al.*, 1994]) was calculated across all longitudes in a 0.5° latitudinal band. To examine seasonal changes in sensitivity of NPP to climate and NDVI, the total annual grid-cell NPP was divided by each annual climate variable or NDVI value and then averaged across each 0.5° latitude band between 60° S and 85° N. Annual values of NDVI are equivalent to the annual integral of NDVI (iNDVI) derived by Schimel *et al.* (1997) as a proxy for annual NPP. The relative importance of climate to simulated NPP was assessed using Spearman Rank correlations (r) between the ratios and individual climate variables across latitudes.

The highest annual NPP estimates for all models occurred in areas with warm (average annual temperature 16° - 27° C) and wet (annual precipitation > 1500 mm) climates and declined as precipitation and temperature decreased (Fig. 18a). The smallest relative variability between model estimates occurred in areas of highest NPP (Fig. 18b), indicating that the best correspondence between model estimates occurred where productivity was least limited by climate, such as in the humid tropics. Although the relative variability was lower in these areas, the absolute variability in NPP among models was not small because NPP estimates were large. Within bands of equal temperature, if temperature was above 10° C, variability between models decreased with increasing precipitation, suggesting that differences in models became less important as water limitations decreased (Fig. 18b). In areas having average temperature below 0° C, variability was generally higher,

suggesting multiple limitations on NPP or very dissimilar effects of low temperature limitation that produced different behavior among models.

Water-use efficiencies within the models were relatively constant across latitudes (Fig 19e), resulting in higher correlations between the latitudinal distribution of NPP and precipitation than with the other climate variables (r = 0.54 - 0.85). The greatest variability among models occurred outside of the wet tropics, indicating that differences in moisture sensitivity became important as precipitation limitation on NPP increased (Fig 15e). Differences among models for temperature sensitivity were greatest in the northern latitudes (50° N - 70° N), i.e. the zone with the shortest active growing seasons (Fig. 19f). Not surprisingly, NPP estimates were strongly correlated with NDVI (r = 0.51 - 0.93), although the magnitude of NPP estimates at any particular NDVI value varied considerably between models. The strong correlations between the latitudinal distributions of NPP and NDVI were also associated with relatively consistent NPP:NDVI ratios across latitudes (Fig. 19h). However, the very high variability in NPP:NDVI around 45° S was associated with higher precipitation coupled with lower NDVI and different modelling strategies, such that CASA, GLO-PEM and TURC estimated much smaller NPP:NDVI ratios compared to other models

Differences in the latitudinal distribution of model sensitivities to climate (Fig. 20) were more conspicuous for monthly than for annual values. The observed uniformity in the latitudinal distribution of annual NPP:Precipitation ratios (Fig. 19e) did not reflect the large seasonal differences in water-use among and within models, demonstrating that similarity in the annual NPP estimates among models does not imply agreement in their distributions of seasonal NPP. For example, the higher sensitivities in the annual NPP:Temperature ratios at northern latitudes above 45° N (Fig. 19f) were detectable as larger monthly ratios during those months when NPP was positive. In contrast, the relatively low and stable annual NPP:Temperature ratios between 30° S and 30° N (Fig. 19f) corresponded with a wide range of NPP responses to temperature, from the consistent monthly ratios in TURC to the extremely large seasonal fluctuations between positive and negative NPP in PLAI and HYBRID (Fig. 20b). Similarly, peaks in annual NPP:Radiation ratios were due to either somewhat higher monthly ratios that changed very little seasonally (between 5° S - 5° N in the tropics) or to larger monthly NPP:Radiation ratios during those months when NPP was positive (between 50° N - 60° N in the north, except for TURC) (Fig. 20C).

Seasonal analyses in the boreal zone revealed that model sensitivities to cold temperatures strongly influenced the timing of phenological onset and offset of the active growing season (Fig. 21). However, different values of NPP were estimated in spring compared to fall for equivalent inputs of a climate variable (i.e. the sensitivity changed), forming an elliptical pattern. Such a pattern is indicative of feedbacks operating within the models that influence the response of NPP to environmental conditions. The different sizes of the ellipsoids indicate that the strength of the feedbacks vary among the models. This influence was also seen as differences in the seasonal pattern of NPP compared to the NDVI, being most pronounced in the beginning and end of the active growing season and in the months of peak productivity. Phenology, in the sense of the seasonally varying display of foliage, may be primarily responsible for the changing relationship between NDVI and solar radiation (Fig. 21). The lower NDVI values during the spring were associated with a dormant or developing canopy whereas the higher NDVI values during late summer/early fall occurred with a fully-developed vegetation canopy. Higher NDVI values from June to August were consistent with increased precipitation and solar radiation, warmer temperatures and a full canopy. This same pattern was reflected, to varying degrees, in the NPP estimates of the models, but the hysteresis between NDVI and NPP in TEM, HRBM and HYBRID indicated that these models did not produce the same canopy dynamics in boreal ecosystems as indicated by the NDVI.

Water balance is most likely responsible for the changing sensitivities of monthly NPP to precipitation and the changing relationship between monthly NDVI and precipitation. During the late spring, the availability of moisture for NPP is very high as melting snow adds water to soils and groundwater so that plants do not have to depend as much on monthly precipitation during this period to support productivity. In contrast, evapotranspiration during the summer depletes soil moisture so that less moisture is generally available for NPP during late summer/early fall and the plants are more dependent upon monthly precipitation. Differences in the elliptical patterns describing the relationship between monthly precipitation and NPP among the models reflect differences in the water balance algorithms used by the models.

In the tropics, sensitivities to climate varied widely among and within models. Seasonal patterns of NPP were more variable among models in the tropics than in the boreal latitudes (Figure 22). The seasonal pattern of NDVI in the tropics corresponded more favorably to monthly precipitation inputs than did simulated NPP, suggesting that the NDVI signal may be more strongly influenced by soil physical properties such as water-holding capacity relative to simulated soil processes.

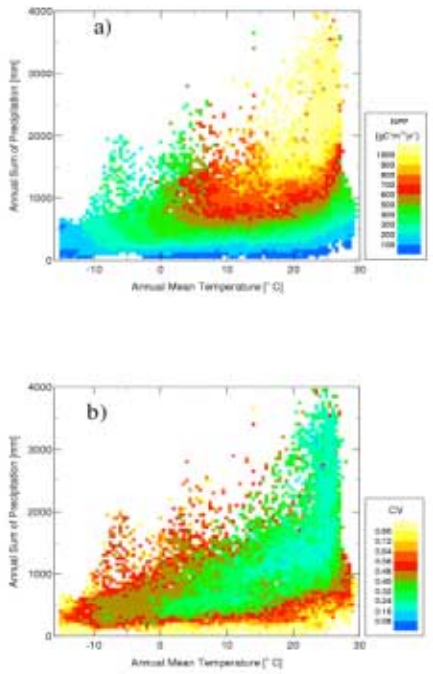

Figure 18: (a) Annual mean net primary production (NPP) for fifteen models in relation to temperature and precipitation; (b) Normalized coefficient of variation for the data shown in panel (a). Data points in both panels represent the mean annual NPP for all models and all grid-cells within a particular temperature- precipitation combination, re-sampled into bins with a temperature interval of 1°C and a precipitation interval of 50 mm yr^{-1}.

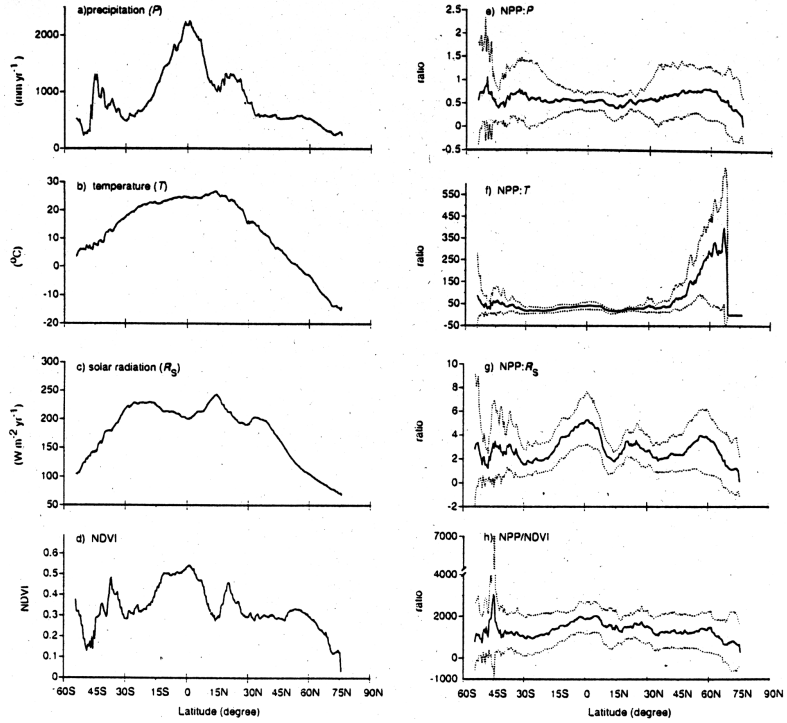

Figure 19: Left panels: Latitudinal distribution of mean values over 0.5° latitudinal bands of a) annual precipitation, b) temperature, c) solar radiation and d) NDVI. Because some land areas were not included in the analysis and data represent only common grid cells, values are somewhat different from those based on all land area. In latitudes dominated by deserts, between 15° N – 30° N, precipitation and NDVI as shown are higher, solar radiation is somewhat lower, while there was no change in temperature than if desert areas had been included. Right panels: Latitudinal distributions of the ratio of annual net primary production to e) total annual precipitation [NPP:*P*], f) average annual temperature [NPP:*T*], g) annual solar radiation [NPP:R_S], and h) average annual NDVI [NPP:NDVI]. Solid lines represent the median ratios for fifteen models within a 0.5° latitudinal band, and dotted lines represent ± 90% confidence intervals of the mean ratios for the models.

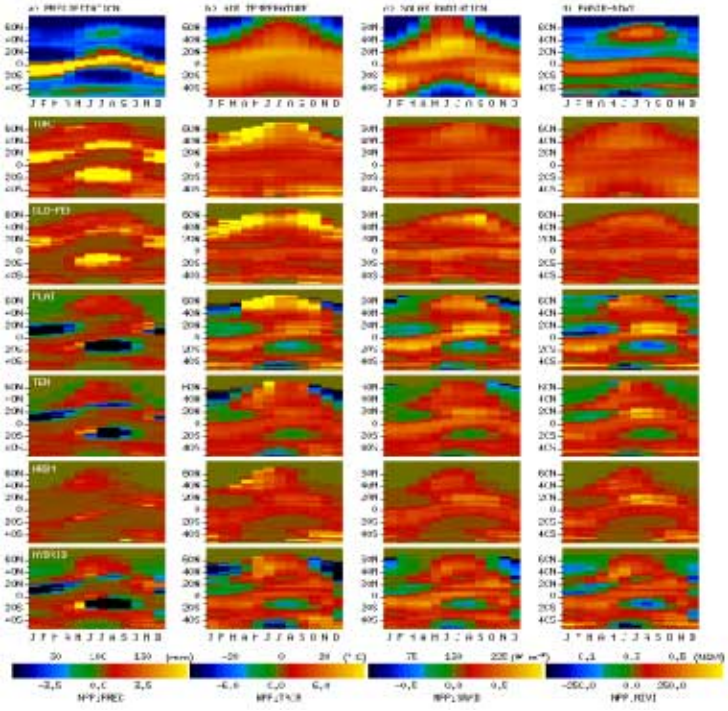

Figure 20: Latitudinal distributions of monthly ratios of simulated net primary productivity to monthly values of a) precipitation [NPP:*P*]; b) temperature in degrees above 0° C [NPP:*T*]; c) solar radiation [NPP:R_s]; and d) NDVI [NPP:NDVI]. Models are shown in descending order by their global NPP estimates. Numbers above the scale-bars represent the values of the climate variable or NDVI plotted on the top panels, and numbers below the scale-bars represent the ratios for the six models plotted on the lower panels.

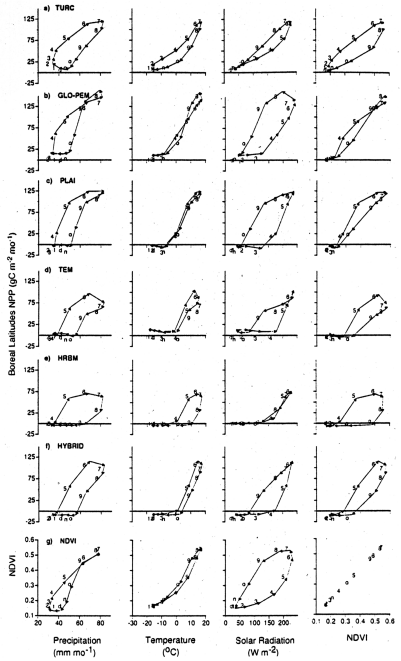

Figure 21: Simulated monthly net primary productivity compared to monthly climate (a-f) and the NDVI (g) averaged over all grid-cells (n = 8266) between 50° N - 60° N. Symbols represent (d) December, (1) January, (2) February; (3) March, (4) April, (5) May; (6) June, (7) July, (8) August, (9) September, (o) October, and (n) November.

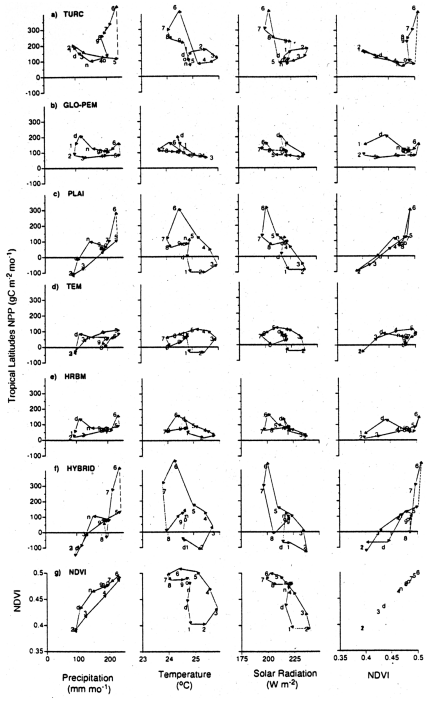

Figure 22: Simulated monthly net primary productivity compared to monthly climate (a-f) and the NDVI (g) averaged over all grid cells (n = 1541) between 0° N- 5° N, the northern half of the highly productive tropical band. Because of differences in seasonality in the tropics above and below the equator, only the northern hemisphere data were used to illustrate the monthly values. NPP values less than -100 gC m^{-2} yr^{-1} in PLAI (-463 in January and -173 in February) and HYBRID (-225 in December, -530 in January and -161 in February) were re-scaled to -100 to fit on the graph. Symbols as for Figure 21.

The changing relationship between NDVI and solar radiation was probably also influenced by phenology, but here, phenology is related to changes in water balance rather than changes in temperature and solar radiation. As very little moisture is stored as snow in the tropics, the availability of soil moisture for NPP is more dependent on the timing of precipitation. Correspondence between NPP and NDVI was generally poor among models, because the pattern of NDVI more strongly reflected monthly inputs of precipitation than did the models. The lag between precipitation and the canopy response shown by the slight elliptical pattern in NDVI compared to precipitation suggests a buffering against water stress by soil moisture storage that was less clear in the models. The distribution of NPP among the models reflected differences in assumptions about the ability of tropical ecosystems to store water. Overall, models estimated higher NPP at larger values of NDVI (and precipitation) than at smaller values, suggesting that month-to-month changes in water availability that were inferred from elevated NDVI values were too slight to be simulated by these models at this spatial and temporal scale.

Differences in model sensitivity to one or more climate variables may not be distinguishable when climate is not limiting or when values are averaged over the year. Despite substantial seasonal differences, models may nevertheless generate comparable annual NPP values over large regions, such as across latitudinal bands, or for the globe, as has been observed for the climatologically (see above) and biophysically (see below) averaged conditions of this intercomparison. Similarities

between model estimates may disappear when climate varies from the average conditions, either as a change in annual averages or as greater amplitude in monthly values.

NPP determines the rate of absorption of atmospheric carbon by land vegetation and model simulations that agree on NPP values may disagree on the underlying processes (e.g., differences in rates of photosynthesis vs. plant respiration, seasonal differences in NPP, differences in light absorption vs. light conversion into dry matter, etc.). This is a cause for concern when the models are applied to scenarios of the future, such as increased atmospheric CO_2 concentration. More important than achieving a consensus on global NPP, therefore, is a better understanding of the processes leading to the net absorption of atmospheric CO_2 by plants, i.e. how plants capture and transform environmental resources to produce dry matter.

Analysis of differences in light absorption and light-use efficiency

Solar radiation is an essential resource for NPP because it is the source of energy that drives the process of photosynthesis. Atmospheric CO_2 is incorporated into dry matter via the consecutive processes of photosynthesis and NPP, each step associated with a yield (or efficiency) of transformation of the solar energy. The methods of Monteith (1972, 1977) were used as a diagnostic tool to understanding how models differed with respect to simulated mechanisms to predict NPP. The assumptions of Monteith (1972, 1977) suggest that geometric factors leading to absorption of solar radiation (e.g., leaf area index, leaf orientation, canopy geometry, leaf optical properties) are relatively independent from biological factors resulting in storing carbon as dry matter by the transformation of absorbed solar energy. Decomposing NPP estimates into geometric (e.g. APAR) and biological (e.g. LUE) factors integrates most mechanistic processes that drive NPP.

Fifteen out of seventeen global models in this intercomparison use solar radiation as a driver of plant production. Twelve global models were compared which: 1) use solar radiation as an input, and 2) either derive directly the fraction of light absorbed by the canopy, or provide the basis to calculate it. The models considered for this analysis were classified into two broad categories according to the way they simulate the absorption of solar radiation and its conversion into dry matter:

For each model, the fraction of light absorbed by plant canopies was estimated by converting incident global radiation provided by the standard data into photosynthetically active radiation (PAR), using a constant ratio of 0.48 MJ(PAR) MJ^{-1}(global radiation) (McCree, 1972). In fact, the models may use a different ratio of PAR to global radiation, or even time- or space-varying ratios. BIOME3, CARAIB, FBM, HYBRID, KGBM, PLAI and SILVAN did not calculate explicitly light absorption at the canopy level, but computed a leaf area index (LAI). For these models, the total fraction of incident PAR absorbed by the canopy was estimated using the Beer-Lambert law, similar to the scheme used in most CPMs in this study to integrate leaf photosynthesis to the canopy. All models provided annual and monthly NPP output. For the eleven models above, plus SIB2 which supplied annual APAR, NPP was decomposed *a posteriori* into absorbed PAR, and conversion of absorbed PAR into dry matter as follows:

$$NPP = (NPP / APAR) * APAR = LUE * APAR \quad \text{(Equation 3)}$$

The relationships between NPP and its components, APAR and LUE, were examined at three spatial levels: 1) grid cell, 2) zonal; and 3) global. For the grid cell level analysis, the values of NPP versus APAR and LUE were plotted for each model over all grid cells of the common area, providing insight into intra-model relationships, or the relationships between NPP and its components within models. At the global scale, global values of NPP versus APAR and LUE were plotted for the twelve models in this study, enabling an analysis of NPP and its components among models. Linear regressions were performed for global and grid cell level plots.

Grid cell level analyses

Correlations between annual NPP and annual APAR at the grid cell level were generally high (Fig. 23), whereas correlations between annual NPP and LUE were weaker (Figure 24), and the intercepts usually departed from zero (e.g., in CASA). Thus, variable NPP estimates within models primarily depended on APAR, and effects of LUE were second order effects.

The high correlations between NPP and APAR and the near-zero intercept for most models, PEMs and CPMs alike, suggest that these models can be, at first order, approximated by a PEM structure, with a constant, model-specific light use efficiency (the slopes of the regression range from 0.39 to 0.52 for the seven highest correlations). Thus, at first glance, the distinction between PEMs and CPMs may not be very important. Similar behavior between CPMs and PEMs may have emerged for several reasons: 1) While the first generation of PEMs may have been less mechanistic than CPMs, refinements introduced to the current generation of PEMs (i.e. stress factors reducing LUE), indicate a developmental convergence with CPMs. 2) The use of a linear light-response curve (in PEMs) versus a saturating curve (in CPMs) may not produce significant differences at the temporal and spatial scales considered as integration in space and time tends to linearize light response curves [*Ruimy et al.*, 1995]. 3) Some CPMs used simplifications (e.g. "optimized Farquhar models" in BIOME3 and SILVAN) that reduced GPP to the product of a light-response curve by other factors, much like PEMs. 4) Although photosynthesis and autotrophic respiration are sensitive to different environmental variables (McCree 1974), at first order, simulated respiration was proportional to GPP.

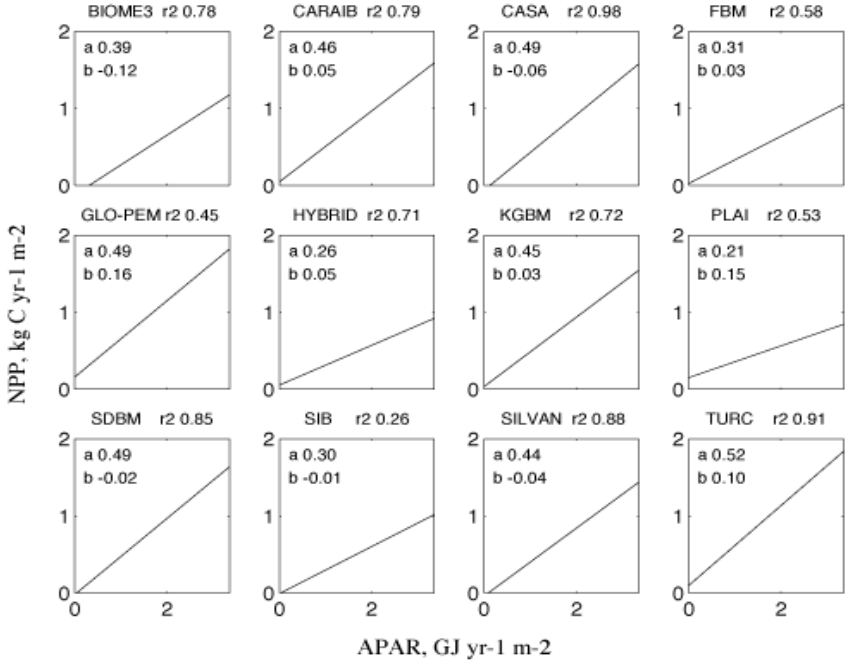

Figure 23: Grid cell level regression of net primary production (NPP) (kg C yr^{-1} m^{-2}) against absorbed photosynthetically active radiation (APAR) (GJ yr^{-1} m^{-2}). Linear correlation coefficient (r^2), slope (a) and intercept (b) are indicated for each model, n=35304.

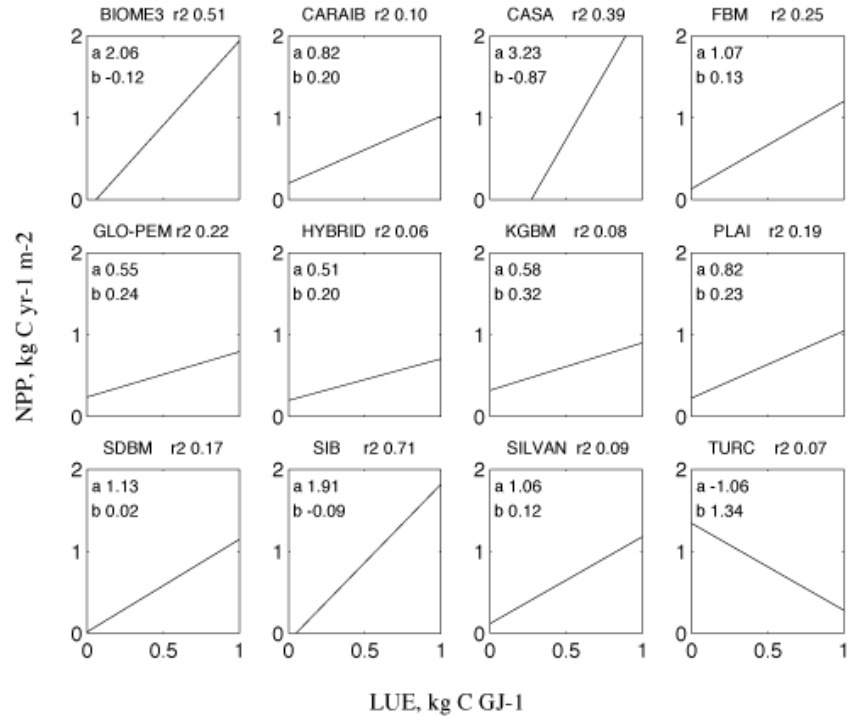

Figure 24: Grid cell level regression of NPP (kg C yr^{-1} m^{-2}) against light use efficiency (LUE) (kg C GJ^{-1}or g C M J^{-1}). Linear correlation coefficients (r^2), slope (a) and intercept (b) are indicated for each model, n=35304.

Global level analyses

In contrast to grid cell level relationships, differences among the models in global NPP estimates did not correspond to differences in global APAR estimates (Fig. 25a). Figure 25a also clearly segregates the models ($P < 0.01$) from NDVI-derived APAR (CASA, GLO-PEM, SDBM, and TURC) from those with modeled APAR (BIOME3, CARAIB, FBM, HYBRID, KGBM, PLAI and SILVAN) where the mean and standard deviation for NDVI-derived modeled APAR were 94×10^{18}; 6.9 J yr^{-1} and 120×10^{18} ; 13.5 J yr^{-1}, respectively. SIB2 was not included in this analysis because incident PAR, being simulated within a coupled General Circulation Model, differed from the data used by the other models. There was a weak, negative correlation ($r = -0.40$) between simulated PAR absorption and NPP and strong, positive correlations with LUE ($r = 0.85$) (Fig. 25b), suggesting that differences in global NPP among models may be due to differences in LUE formulations.

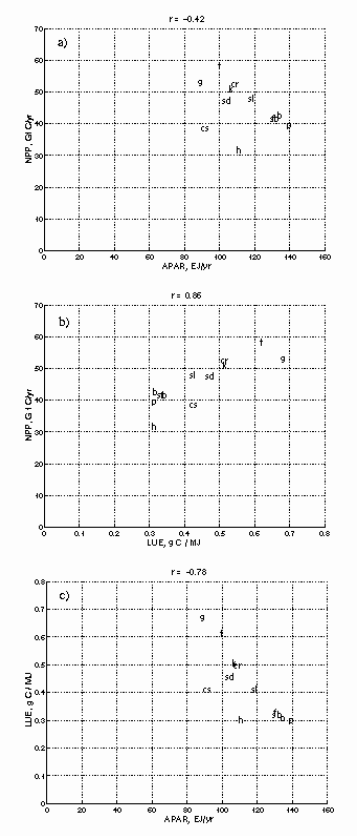

Figure 25: Global level regressions. (a) Global NPP (Pg C yr^{-1}) against mean global APAR (10^{18} J yr^{-1}); (b) Global NPP (Pg C yr^{-1}) against mean LUE (g C MJ^{-1}); (c) Global LUE (g C MJ^{-1}) against mean global APAR (10^{18} J yr^{-1}). Linear correlation coefficients (*r*) are indicated. The models are: BIOME3 (b), CARAIB (cr), CASA (cs), FBM (f), GLO-PEM (g), HYBRID (h), KGBM (k), PLAI (p), SDBM (sd), SIB2 (sb), SILVAN (sl), and TURC (t).

The strong negative correlation between LUE and APAR (Fig 25c) suggested that estimates of global NPP among models were relatively constant (see Eq. 3), either by explicit or unconscious adjustment of parameters within models with the consequence that global results were within a commonly accepted range. The fact that these models could be calibrated puts a damper on the confidence that we may have in global models of NPP, confidence resulting from the fact that global estimates have changed little since Lieth (1975) estimated global NPP to be around 60 Pg C yr^{-1}. On the other hand, many models were conceived as tools for formalizing the complex relationships between NPP and forcing factors, rather than estimating the absolute value of NPP.

Some models explicitly calibrated certain parameters with values of either global NPP, or NPP per biome. For instance, CASA calibrated a globally uniform value of optimum LUE in the absence of any environmental stresses, using NPP data for about 20 sites. Historically, only a limited number of compilations of NPP exist per biome, for instance the Whittaker and Likens (1975) estimates were used to calibrate and evaluate current models.

Zonal profiles

NPP and APAR shared the same double-peak pattern (Figures 26a and 26b), while latitudinal variations of LUE were smaller (Figure 26c), and the same order of magnitude for inter-model variability. Thus, the analysis of zonally averaged factors was another indication that variations of NPP within models were determined by APAR on a first order, while variations of NPP among models were determined by LUE. GLO-PEM was an exception, as it presented obvious maxima for mid- to high-latitudes, and minima for the seasonal tropics, much like the latitudinal variations of NPP and APAR. Only in GLO-PEM is LUE a significant factor in explaining spatial variations of NPP.

The "resource balance perspective" (Field *et al.* 1995) provides insight into understanding why models with a very different structure may predict similar patterns of APAR. This hypothesis suggests that all environmental resources should be equally limiting to growth such that plants do not harvest more light than they can utilize for growth. As a consequence, APAR should be related to whatever resource limits growth. In addition, soil nutrients and ecosystem structure adjust in response to climate over long time scales [*Jenny*, 1941]. Thus, whatever the general approach used in the NPP model, i.e. whether NPP is determined primarily by climate, nutrient availability or vegetation type, similar spatial patterns of APAR are expected. In fact, two global models out of seventeen in the intercomparison did not use solar radiation as a driver of plant production (see Introduction, above). The main conceptual approach could be statistical relationships between production and climate variables, temperature and precipitation for instance, or relationships between carbon assimilation and nutrient availability. Even the outputs from these models did not generally depart significantly from the models analyzed here.

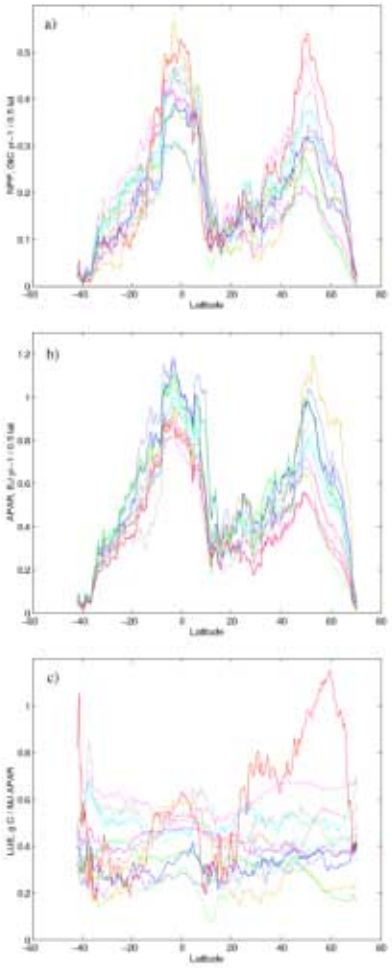

Figure 26: Zonal profiles per 0.5° latitude zones. (a) NPP (Pg C yr^{-1} 0.5° $(lat)^{-1}$); (b) APAR (MJ yr^{-1} 0.5° $(lat)^{-1}$); (c) LUE (g C MJ^{-1}). The models are: BIOME3 (solid green), CARAIB (solid light blue), CASA (solid purple), FBM (solid dark blue), GLO-PEM (solid red), HYBRID (dashed green), KGBM (dashed grey), PLAI (dashed dark blue), SDBM (dashed red), SIB2 (solid yellow), SILVAN (dashed light blue), and TURC (dashed purple).

The zonal profiles were a qualitative assessment of variable response (NPP and its drivers) over environmental gradients (such as water and temperature). The primary effect of limitations in available resources is to reduce APAR (Fig. 26a ,b), while effects on LUE were secondary. Some features are more or less constant in the zonal profiles of LUE (Fig. 26c). In the dry tropics (15° - 25° N), all models exhibited a dip in LUE, reflecting a water shortage. In the equatorial zone (0° - -10°), all models, except TURC, predicted a peak in LUE, reflecting the abundance of environmental resources available for plant production (water, light, nitrogen). This can be explained for all models, except TURC, where simulated stress factors resulted in a reduction of LUE when water, and sometimes also nitrogen, were limiting. Important discrepancies among models were visible in Northern temperate and boreal zones (30° - 60° N). Mean values of LUE were the most variable in these latitudes, primarily because of the extremely high LUE for GLO-PEM. In addition, the temperature gradient which characterized this zone corresponded to either a strong increase (GLO-PEM), a slight increase (HYBRID, TURC, SDBM, PLAI), no significant trend (CARAIB, CASA, FBM, KGBM, SILVAN), or a decrease in LUE (BIOME3). Thus, models generally agreed on the effects of water stress on light use efficiency, but did not agree on the effects of temperature.

Reducing the uncertainty in APAR

Spatial patterns of APAR were very similar among models. The main difference was in the overall value of APAR: the NDVI-derived APAR was significantly lower than modeled APAR. The following suggest different possible reasons behind the consistent global 28% discrepancy:

Underestimation of NDVI-derived FPAR: The NDVI product was pre-processed with atmospheric corrections, calibration, filtering, compositing, and reconstruction where cloud contamination is known to be particularly important (Sellers *et al.* 1994). The effect of most of the contamination was to decrease the satellite signal compared to what could be measured at the surface. Some additional cloud, atmospheric or instrumental contamination may remain after processing (Ouadrari *et al.* 1997). However, the various algorithms used to calibrate the FPAR/NDVI relationship assumed that maximum FPAR (in the range 0.9-0.98 depending on the model) corresponded to maximum NDVI, which should correct some of the remaining underestimation of the satellite signal.

Overestimation of modeled FPAR : Some models might overestimate LAI because they did not include the entire range of possible constraints on LAI: there was no upper limit, for instance, on the LAI of KGBM provided there was enough water. In addition, some models calibrated some of their relationships such that maximum LAI agreed with the literature data, but these data generally come from more productive stands, which could be biased towards high values, and not representative of a 0.5° longitude/latitude grid cell area.

Potential versus actual land cover: Satellite-derived FPAR corresponded to actual land cover including natural, agricultural and urban areas, while models that computed LAI usually considered potential natural vegetation. Potential vegetation generally has higher FPAR than agricultural and urban areas. Even though crops develop a very dense canopy and the resulting APAR could be of the same order as natural vegetation, the active period was shorter for crops compared to grassland or deciduous forests. Results from CARAIB, however, which computed LAI but did incorporate land use, did not support this hypothesis. In regions with little or no land use, simulated APAR from CARAIB were generally closer to satellite-derived APAR than other models simulating LAI, but in regions which were strongly affected by land use, its simulated APAR remained higher than the satellite-derived APAR (not shown).

Presently, it is not possible to determine which of these possible reasons was the primary cause of the discrepancies. An answer to this question will likely come from improved remote sensing and modelling techniques. In the last decade, NDVI derived from NOAA-AVHRR has been the only reliable source of satellite data available to monitor the activity of vegetation from space. New sensors (POLDER, VEGETATION, MODIS, etc.), having increased spatial resolution as well as spectral and directional properties, will provide improved land cover estimates and vegetation properties, including FPAR.

Reducing the uncertainty in LUE
Differences in NPP among models were determined by differences in LUE. Light use efficiencies supposedly varied within a narrow range (e.g., Monteith 1972, 1977), so they could be considered a "characteristic" of a vegetation type or a climatic zone. In addition, LUE was not a variable used explicitly in the CPMs. Thus, values of LUE derived from the literature could constitute an independent check of model behavior.

The comparison with literature data was limited here to the overall range of variation, not exact grid cell by grid cell values or even means per biomes. Indeed, many other factors, apart from model errors could generate discrepancies between simulated and measured light use efficiencies: 1) differences in the definition of biomes (see ecotones, above); 2) differences in the definition of light-use efficiencies (for instance, literature-derived LUE generally corresponded to above-ground LUE, while model values corresponded to total LUE); and 3) sampling biases in the literature data (because of the scarcity of data, the values corresponding to mean per biomes were generally not representative). More information will come from the development of improved techniques for measuring fluxes of CO_2 over whole canopies. From these measurements, it will be generally possible to extract light use efficiencies for GPP that are more representative of entire ecosystems and their seasonal variations [*Ruimy et al.*, 1995].

Conclusions

This first systematic comparison of terrestrial biogeochemical models was performed using the terrestrial carbon flux variable (NPP). Results have shown generally good agreement between the present generation of models over many broad features, despite the fact that the models had been developed for widely differing purposes and with widely differing resource bases for personnel and computing power. However, and perhaps more interestingly, both the differences in model behavior and the unresolved question of explicit or unconscious calibration to an assumed global NPP have highlighted potentially important shortcomings in our understanding of the total Earth system. These issues need to be resolved if the demands (e.g. Kyoto Protocol, 1988) for predictions or sensitivity assessments of the stability and sustainability of the terrestrial biosphere are to be credible. Improved physical models of the ocean and atmosphere alone cannot improve the predictability of the Earth's system carbon-exchange processes. Moreover, a recent assessment of the future of coupled systems [*Melillo et al.*, 1996] indicated that atmospheric and oceanic simulations are likely to be highly sensitive to the dynamics of the terrestrial biosphere.

Recently, new technological and scientific developments have indicated that our ability to observe changes in biospheric activity may be greater than anticipated. Keeling *et al.* (1996) made the convincing point that at least over the period since 1960, biospheric activity in northern latitudes may have changed strongly enough to produce an average extension of the growing period by seven days. Myneni *et al.* (1997) used the AVHRR satellite record to confirm this result, while also indicating the regional uncertainties. The modelling teams aiming at simulating global carbon fluxes now face the challenge to explain or reject these and other hypotheses about the dynamics of the Earth's vegetation.

To meet this challenge, several activities are now underway—some of them being spawned from the NPP workshops:

• Numerous ‘minor findings’ from the working group discussions have already lead to improved versions of the various models. In several cases, only the thorough scrutiny provided by colleagues during the comparison process could identify errors or minor inadequacies that have initiated model improvement.

• The importance of an improved data basis for several key features of model development and application has been illustrated and is now leading to accelerated activities in several key areas, such as climate [*Cramer*, 1996; *Cramer et al.*, 1996], soils [*Scholes*, 1996], and land use [*Turner et al.*, 1995]. A particular area where better data products are achievable and urgently needed is the wealth of site-based observations of biogeochemical fluxes. As a direct spin-off from the Potsdam comparisons, an international team, the Global Primary Production Data Initiative (GPPDI) is now developing a new collection of such observed variables, as well as improved methods to make this data useful at the broad scale required for global applications [*Olson and Prince*, 1996, [Scurlock, accepted into EA #5734; *Prince et al.*, 1995].

APPENDIX 1

VALIDATING NPP SIMULATIONS WITH THE IGBP TERRESTRIAL TRANSECTS

The developing set of IGBP terrestrial transects offers an excellent opportunity to validate simulations of NPP from the various global models. The transects are defined as a series of study sites distributed along an underlying gradient of a major environmental factors (e.g., temperature, precipitation) that influence ecosystem structure and function. The spatial context in which the study sites are located is also important. In most cases the underlying environmental gradients are sufficiently orderly to support an approximately linear gradient in physical space, and are physically contiguous. The length of the transects has been specified as of the order of 1000 km, to ensure that they overlap sufficiently with the spatial realm of global climate, atmospheric, and biospheric models. The transects do not have a prescribed width, but it is often fixed to facilitate the application of remotely sensed data.

The transect studies involve both extensive, coarse-grain studies and intensive, patch-scale experimental studies at selected sites along the transects. The intensive studies will be particularly important in examining fine-scale heterogeneity that is of special significance for certain processes, for example, the controls on NPP by local-scale soil factors. An important part of the transect studies is the extrapolation of the understanding gained from intensive patch-scale studies at key points along the transect to landscape and regional levels. The strategy proposed to achieve this involves a hierarchy of observations (tower, aircraft and remote sensing measurements) and models (patch-scale process models, landscape models, global models).

The proposed initial IGBP Terrestrial Transects are located in four key regions, identified on the basis of their likelihood to be altered by components of global change and the strength of their potential feedbacks to global change. These are: (1) humid tropical systems undergoing land-use change; (2) high latitude regions extending from boreal forest into tundra; (3) semi-arid tropical regions from dry forest or shrubland to grasslands; and (4) mid-latitude semi-arid regions encompassing transitions from forest or shrublands to grasslands. Within each of these regions, a distribution of transects between hemispheres and continents is desirable.

The transects offer the ideal testbed for global models such as those simulating NPP. The advantages of the transects include:

• they are at an appropriate scale for testing global models (i.e., they encompass sufficient pixels for 0.5^{o} x 0.5^{o} based models).

• they are designed specifically to address the scaling issue, so that they can extrapolate small-scale process understanding and local heterogeneity to scales of value to global models.

• they provide a broad base of background ecological data (e.g., soils, climate, vegetation composition, above-ground biomass, sub-grid scale distribution of veg types, etc.) that can assist in the parameterisation of models and in the interpretation of model results.

• they are based on gradients (temperature, precipitation, land-use) that are directly applicable to global change studies. These are the parameters that will most influence changes to terrestrial NPP over the coming decades.

Thus, the transects are in an excellent position to provide the basis for the next steps in the NPP model intercomparison project. We propose that the suite of models that participated in the Potsdam 95 intercomparison be run for the set of IGBP Terrestrial Transects, both with present climate and with an agreed future scenario. The transects are various stages of development, so that for some transects (e.g. SALT, Great Plains, China, Alaska) there is already considerable data available for validation. For others, (e.g. NATT, Canada, Kalahari) data will soon be available. Some are still in the conceptual stage, but even here, the NPP simulations for the regions proposed for the transects may stimulate more rapid development of them, including guidance for the location of sites and the types of measurements which need to be made.

REFERENCES

Agbu, P.A., and M.E. James, The NOAA/NASA Pathfinder AVHRR Land Data Set User's Manual, Goddard Distributed Active Archive Center, NASA, Goddard Space Flight Center, 1994.

Berthelot, B., G. Dedieu, F. Cabot, and S. Adam, Estimation of surface reflectances and vegetation index using NOAA/AVHRR: methods and results at global scale., pp. 33-40, Val d'Isere, 1994.

Bolin, B.B., E.T. Deegens, S. Kempe, and P. Ketner, The global carbon cycle, New York, 1979.

Bolin, B.B., B.R. Doos, J. Jager, and R. Warrick, *The Greenhouse Effect, Climate Change, and Ecosystems*, 541 pp., John Wiley & Sons, Chichester, 1986.

Burke, I.C., T.G.F. Kittel, W.K. Lauenroth, P. Snook, C.M. Yonker, and W.J. Parton, Regional analysis of the Central Great Plains: Sensitivity to climate variability, *BioScience*, *41*, 685-692, 1991.

Chen, J.M., Optically-based methods for measuring seasonal variation of leaf area index in boreal conifer stands, *Agricultural and Forest Meteorology*, *80*, 135-163, 1996.

Churkina, G., S.W. Running, and A. Schloss, Comparing global models of terrestrial net primary productivity (NPP): The importance of water availability to primary productivity, 1995.

Ciais, P., P. Tans, J. White, M. Trolier, D. Schimel, and others, Partitioning of Ocean and Land Uptake of CO2 as Inferred by Delta-C-13 Measurements from the NOAA Climate Monitoring and Diagnostics Laboratory Global Air Sampling Network, *J. Geophys. Res.*, *100*, 5051-5070, 1995.

Cramer, W., IGBP Newsletter, Workshop on globally gridded historical climate data sets for biosphere models., 1996.

Cramer, W., M. Hutchinson, R. Leemans, and B. Huntley, A new climate data base for terrestrial ecosystem modelling with variable spatial resolution, in prep.

Cramer, W., and R. Leemans, *Assessing impacts of climate change on vegetation using climate classification systems*, Vegetation Dynamics and Global Change, 190-217 pp., Chapman and Hall, New York, 1993.

Cramer, W., B. Moore, and D. Sahagian, Data needs for modelling global biospheric carbon fluxes - lessons from a comparison of models. IGBP Newsletter, 1996.

Dorman, J., and P. Sellers, A global climatology of albedo, roughness length and stomatal resistance for Atmospheric General Circulation Models as represented by the Simple Biosphere Model (SiB), *Journal of Applied Meteorolgy*, *28*, 833-855, 1989.

Dye, D., and R. Shibasaki, Intercomparison of Global PAR Data Sets, *Geophysical Research Letters*, *22*, 2013-2016, 1995.

Esser, G., and M. Lautenschlager, Estimating the Change of Carbon in the Terrestrial Biosphere from 18000 BP to Present Using a Carbon Cycle Model, *Environ. Pol.*, *83*, 45-53, 1994.

FAO/UNESCO, Soil Map of the World, 1:5000000, v. VI (Africa), UNESCO, Paris, 1977.

Farquhar, G.D., S.v. Caemmerer, and J.A. Berry, Biochemical model of photosynthetic CO_2 assimilation in leaves of C_3 species, *Planta*, *149*, 78-90, 1980.

Field, C., J. Randerson, and C. Malmstrom, Global net primary production: combining ecology and remote sensing, *Remote Sensing of Environment*, *51*, 74-88, 1995.

Friend, A., and P. Cox, Modelling the effects of atmospheric CO2 on vegetation-atmosphere interactions, *Agricultural and Forest Meteorology*, *73*, 2850295, 1995.

Friend, A.D., Parameterisation of a global daily weather generator for terrestrial ecosystem and biogeochemical modelling, *Ecological Modelling*, in press.

Friend, A.D., A.K. Stevens, R.G. Knox, and M.G.R. Cannell, A process-based, terrestrial biosphere model of ecosystem dynamics (Hybrid v. 3.0), *Ecological Modelling*, 249-287, 1997.

Fung, I., C. Tucker, and K. Prentice, Application of very high resolution radiometer vegetation index to study atmosphere biosphere exchange of CO2., *J. Geophys. Res.*, *92*, 2999-3015, 1987.

Gallo, K., Experimental global vegetation index from AVHRR utilizing pre-launch calibration, cloud and sun angle screening, Digital Data, Boulder, 1992.

Gholz, H.L., Environmental Limits on Aboveground Net Primary Production, Leaf Area, and Biomass in Vegetation Zones of the Pacific Northwest, *Ecology*, *63*, 469-481, 1982.

Goward, S., and K. Huemmrich, Vegetation canopy PAR absorptance and the Normalized Difference Vegetation Index: An assessment using the SAIL model., *Remote Sensing of Environment*, *39*, 119-140, 1992.

Grier, C.C., and S.W. Running, Leaf area of mature north-west coniferous forests: relation to site water balance, *Ecology*, *58*, 893-899, 1977.

Haxeltine, A., and I. Prentice, BIOME3: an equilibrium biosphere model based on ecophysiological constraints, resource availability and competition among plant functional types, *Glob. Biogeochem. Cycles*, *10*, 693-710, 1996.

Haxeltine, A., I.C. Prentice, and I.D. Cresswell, A Coupled Carbon and Water Flux Model to Predict Vegetation Structure, *Journal of Vegetation Science*, *7*, 651-666, 1996.

Heimann, M., The TM2 tracer model, model description and user manual, *Deutsches Klimarechenzentrum*, *10*, 47, 1995.

Heimann, M., G. Esser, B. Moore, A. Haxeltine, R. Otto, J. Kaduk, I. Prentice, D. Kicklighter, W. Sauf, W. Knorr, A. Schloss, G. Kohlmaier, S. Sitch, A. McGuire, U. Wittenberg, J. Melillo, and G. Wurth, Evaluation of terrestrial carbon cycle models through simulations of the seasonal cycle of atmospheric CO2: First results of a model intercomparison study, *submitted Glob. Biogeochem. Cyc.*, in press.

Heimann, M., and C. Keeling, A three-dimensional model of atmospheric CO2 transport based on observed winds: 2. Model description and simulated tracer experiments, in *Aspects of Climate Variability in the Pacific and Western Americas*, D.H. Peterson, pp. 237-275, 305-363, Amer. Geophys. U., Washington D.C., 1989.

Heimann, M., and P. Monfray, Spatial and temporal variation of the gas exchange coefficient for CO2: 1. Data Analysis and Global Validation, Max Planck Institut fur Meteorologie, Hamburg, Germany, 1989.

Houghton, J.T., L.G.M. Filho, B.A. Callandar, N. Harris, A. Kattenberg, and K. Maskell, *Climate Change 1995: Contribution of Working Group 1 to the Second Assessment Report of the Intergovernmental Panel on Climate Change.*, Climate Change 1995: The Science of Climate Change, 572 pp., Cambridge University Press, new York, 1995.

Hubert, B., L. Francois, P. Warnant, and D. Strivay, Stochastic generation of meteorological variables and effects on global models of water and carbon cycles in vegetation and soils, *Journal of Hydrology*, in press.

Hulme, M., Rainfall changes in Africa: 1931-1960 1961-1990, *International Journal of Climatology*, *12*, 685-699, 1992.

Hungerford, R., R. Nemani, S. Running, and J. Coughlan, A Mountain Microclimate Simulation Model, *Intermt. Res. Sta., For. Serv., USDA Res. Pap*, 1989.

Jarvis, P., and J. Leverenz, Productivity of temperate, deciduous and evergreen forests, *Physiological Plant Ecology*, 234-280, 1983.

Jenny, H., *Factors of soil formation*, , McGraw-Hill, New York, 1941.

Kaduk, J., and M. Heimann, A prognostic phenology scheme for global terrestrial carbon cycle models, *Climate Research*, *6*, 1-19, 1996.

Keeling, C., J. Chin, and T. Whorf, Increased activity of northern vegetation inferred from atmospheric CO2 measurements, *Nature*, *382*, 146-148, 1996.

Kergoat, L., A model of hydrologic equilibrium of leaf area index at the global scale., *Journal of Hydrology*, in press.

Kindermann, J., M.K.B. Ludeke, F.W. Badeck, R.D. Otto, A. Klaudius, C. Hager, G. Wurth, T. Lang, S. Donges, S. Habermehl, and G.H. Kohlmaier, Structure of a Global and Seasonal Carbon Exchange Model for the Terrestrial Biosphere, *Water, Air, and Soil Pol.*, *70*, 675-684, 1993.

Kindermann, J., G. Wurth, G.H. Kohlmaier, and F.W. Badeck, Interannual variation of carbon exchange fluxes in terrestrial ecosystems, *Glob. Biogeochem. Cycles*, *10*, 737-756, 1996.

Knorr, W., and M. Heimann, Impact of Drought Stress and Other Factors on Seasonal Land Biosphere CO2, Exchange Studied Through an Atmospheric Tracer Transport Model, , *47*, 471-489, 1995.

Kohlmaier, G.H., F.W. Badeck, R.D. Otto, C. Hager, S. Donges, J. Kindermann, G. Wurth, T. Lang, U. Jakel, A. Nadler, P. Ramge, A. Klaudius, S. Habermahl, and M.K.B. Ludeke, The Frankfurt Biosphere Model: a global process-oriented model of seasonal and long-term CO2 exchange between terrestrial ecosystems and the atmosphere.II. Global results for potential vegetation in an assumed equilibrium state, *Climate Research*, *8*, 61-87, 1997.

Kuchler, A., World map of natural vegetation, in *Goode's World Atlas*, , pp. 16-17, Rand McNally, 1983.

Kumar, M., and J. Monteith, Remote sensing of crop growth, in *Plants and the daylight spectrum*, H. Smith, pp. 133-144, Acad. Press, N.Y., 1981.

Landsberg, J., *Physiological Ecology of Forest Production*, 198 pp., Academic Press, London, 1986.

Leemans, R., and W. Cramer, The IIASA database for mean monthly values of temperature, precipitation, and cloudiness on a global terrestrial grid, IIASA, 1991.

LeRoux, X., H. Gauthier, A. Begue, and H. Sinoquet, Radiation absorption and use by humid savannah grassland: assessment using remote sensing and modelling, *Agricultural and Forest Meterology*, *85*, 117-132, 1997.

Lieth, H., Modelling the primary production of the world, in *Primary Productivity of the Biosphere*, H. Lieth, and R.H. Whittaker, pp. 237-263, Springer-Verlag, 1975.

Los, S., C. Justice, and C. Tucker, A global 1 degree-by 1 degree NVDI data set for climate studies derived from the GIMMS continental NDVI data, *International Journal of Remote Sensing*, *15*, 3493-3518, 1994.

Ludeke, M., F. Badeck, and R. Otto, The Frankfury Biosphere Model. A global process oriented model for the seasonal and long-term CO2 exchange between terrestrial ecosystems and the atmosphere. I. Model description and illustrative results for cold deciduous and boreal forests, *CLimate Research*, *4*, 143-166, 1994.

Maisongrande, P., A. Ruimy, G. Dedieu, and B. Saugier, Monitoring seasonal and interannual variations of gross primary productivity, net primary productivity and net ecosystem productivity using a diagnostic model and remotely-sensed data., *Telbus Series B- Chemical and Physical Meteorology*, *47B*, 178-190, 1995.

Malmstrom, C., J. Randerson, M. Thompson, H. Mooney, and C. Field, The next dimension: extending the time axis of global NPP estimates, in *Photosynthesis and Remote Sensing, Satellite Meeting of the 10th International Congress of Photosynthesis*, G. Guyot, pp. 407-411, EARSeL-INRA, Montpellier, 1995.

Matthews, E., Global vegetation and land use: New high-resolution data bases for climate studies, *Journal of Climate and Applied Meteorology*, *22*, 474-487, 1983.

McCree, K.J., The action spectrum, absorptance and quantum yield of photosynthesis in crop plants, *Agricultural Meteorology*, *9*, 191-216, 1972.

McCree, K.J., Equation for the rate of dark respiration of white clover as function of dry weight, photosynthesis rate and temperature, *Crop Science*, *14*, 509-514, 1974.

McGuire, A., J. Melillo, and D. Kicklighter, Equilibrium responses of soil carbon to climate change - empirical and process based estimates, *Journal of Biogeography*, *22*, 785-796, 1995.

McGuire, A., J. Melillo, and D. Kicklighter, The role of the nitrogen cycle in the global response of net primary production and carbon storage to doubled CO2, *Global Biogeochemical Cycles*, in press.
Meeson, B., F. Corpew, and J. McManus, Initiative I-global Data Sets for Land-atmosphere Models, NASA, 1995.
Melillo, J., I. Prentice, G. Farquhar, E. Schulze, and O. Sala, Terrestrial Biotic Responses to Environmental Change and Feedbacks to Climate, in *Climate Change 1995- The Science of Climate Change*, J. Houghton, L.M. Filho, B. Callander, N. Harris, A. Kattenberg, and K. Maskell, pp. 445-481, Cambridge University Press, Cambridge, 1996.
Melillo, J.M., A.D. McGuire, D.W. Kicklighter, B.M. III, C.J. Vorosmarty, and A.L. Schloss, Global climate change and terrestrial net primary production, *Nature*, *363*, 234-240, 1993.
Members, V., J. Melillo, and J. Borchers, Vegetation/ecosystem modelling and analysis project: Comparing biogeograpy and biogeochemistry models in a continental-scale study of terrestrial ecosystem responses to climate change and CO2 doubling, *Global Biogeochemical Cycles*, *9*, 407-437, 1995.
Monteith, J., Climate and the efficiency of crop production in Britain, *Royal Society of London, Philosophical Transaction*, *281*, 277-294, 1977.
Monteith, J.L., Solar radiation and productivity in tropical ecosystems, *Journal of Applied Ecology*, *9*, 747-766, 1972.
Moore III, B., R. Boone, J. Hobbie, R. Houghton, J. Melillo, B. Peterson, G. Shaver, C. Vorosmarty, and G. Woodwell, A simple model for analysis of the role of terrestrial ecosystems in the global carbon budget, in *Modelling the global carbon cycle*, B. Boiln, pp. 365-385, Wiley, N.Y., 1981.
Moore III, B., and B. Braswell, The Lifetime of Excess Atmospheric Carbon Dioxide, *Global Biogeochemical Cycles*, *8*, 23-38, 1994.
Moulin, S., L. Kergoat, N. Viovy, and G. Dedieu, Global scale assessment of vegetation phenology using NOAA/AVHRR satellite measurements, *Journal of Climate*, in press.
Myneni, R.B., C.D. Keeling, C.J. Tucker, G. Asrar, and e. al., Increased plant growth in the northern high latitudes from 1981 to 1991, *Nature*, *386*, 698-702, 1997.
Neilson, R., G. King, and G. Koerper, Toward a rule-based biome model, *Landscape Ecol.*, *7*, 27-43, 1992.
Nemry, B., L. Francois, P. Warnant, F. Robinet, and J. Gerard, The seasonality of the CO2 exchange between the atmosphere and the land biosphere: A study with a global mechanistic vegetation model, *Journal of Geophysical Research*, *101*, 7111-7125, 1996.
Nepstad, D., and n. others, The role of deep roots in the hydrological and carbon cycles of Amazonian forests and pastures, , *372*, 666-669, 1994.
Olson, D., and S. Prince, Global primary production data initiative update, *IGBP Newsletter*, *27*, 13, 1996.
Olson, J., J. Watts, and L. Allison, Major World Ecosystem Complexes Ranked by Carbon in Live Vegetation: A Database, Carbon Dioxide Information Center, 1985.
Otto, R., E. Hunt, and G. Kohlmaier, Static and dynamic input data of Terrestrial Biogeochemical Models, *Global Biogeochemical Cycles*, manuscript.
Ouadrari, H., E. Vermote, N.E. Saleous, and D. Roy, AVHRR Pathfinder II dataset: Evaluation and improvements, in *7th International Symposium on Physical Measurements and Signatures in Remote Sensing*, Courchevel, France, 1997.
Pan, Y., A. McGuire, D. Kicklighter, and J. Melillo, The importance of climate and soils for estimates of ne primary production-a sensitivity analysis with the terrestrial ecosystem model, *Global Change Biology*, *2*, 5-23, 1996.
Parton, W., J. Scurlock, and D. Ojima, Observations and modelling of biomass and soil organic matter dynamics for the grassland biome worldwide, *Global Biogeochemical Cycles*, *7*, 785-809, 1993.
Plochl, M., and W. Cramer, Coupling global models of vegetation structure and ecosystem processes, *Tellus*, *47B*, 240-250, 1995a.
Plochl, M., and W. Cramer, Possible impacts of global warming on tundra and boreal forest ecosystems-comparison of some biogeochemical models, *Journal of Biogeography*, *22*, 775-784, 1995b.
Post, W., J. Pastor, P. Zinke, and A. Stangenberger, Global patterns of soil nitrogen storage, *Nature*, *317*, 613-616, 1985.
Post, W.M., T.H. Peng, W.R. Emanuel, A.W. King, and others, The Global Carbon Cycle, *Amer. Sci.*, *78*, 310-326, 1990.
Potter, C., J. Randerson, C. Field, P. Matson, P. Vitousek, H. Mooney, and S. Klooster, Terrestrial ecosystem production-a process model based on global satellite and surface data, *Global Biogeochemical Cycles*, *7*, 811-841, 1993.
Prentice, I.C., W. Cramer, S. Harrison, R. Leemans, and others, A global biome model based on plant physiology and dominance, soil properties and climate, *J. Biogeogr.*, *19*, 117-134, 1992.
Prentice, I.C., and T.W. III, Global Palaeovegetation Data for Climate-Biosphere Model Evaluation, *GAIM Report Series*, *in press*, 1996.
Priestley, C.H.B., and R.J. Taylor, On the assessment of surface heat flux and evaporation using large-scale parameters, *Monthyly Weather Review*, *100*, 81-92, 1972.
Prince, S., A model of regional primary production for use with coarse-resolution satellite data, *International Journal of Remote Sensing*, *12*, 1313-1330, 1991.
Prince, S., and S. Goward, Global net primary production: a remote sensing approach, *Journal of Biogeography*, *22*, 815-835, 1995.
Prince, S., R. Olson, G. Dedieu, G. Esser, and W. Cramer, Global Primary Production Data Initiative Project Description, IGBP DIS, 1995.
Randall, D., P. Sellers, and J. Berry, A revised land surface parameterization (SiB2) for atmospheric GCMs. Part III: The greening of the Colorado State University General Circulation Model, *Journal of Climate*, *9*, 738-763, 1996.

Rosenzweig, M.L., Net primary productivity of terrestrial communities: prediction from climatological data, *The American Naturalist*, *102*, 67-74, 1968.
Ruimy, A., G. Dedieu, and B. Saugier, TURC: a diagnostic model of continental gross primary productivity and net primary productivity., *Global Biogeochemical Cycles*, *10*, 269-286, 1996.
Ruimy, A., L. Kergoat, and A. Bondeau, Comparing global models of terrestrial net primary productivity(NPP): Analysis of differences in light absorption, light-use efficiencey, and whole respiration cost., 1995.
Running, S., R. Nemani, and R. Hungerford, Extrapolation of synoptic meteorological data in mountainous terrain, and its use for simulating forest evapotranspiration and photosynthesis, *Canadian Journal of Forest Research*, *17*, 472-483, 1987.
Running, S.W., and E.R. Hunt, Generalization of a forest ecosystem process model for other biomes, BIOME-BGC and an application for global-scale models, in *Scaling Physiological Processes: Leaf to Globe*, J. Ehleringer, and C. Field, pp. 1410158, Academic Press, San Diego, 1993.
Schimel, D., Terrestrial Ecosystems and the Carbon Cycle, *Glob. Change Bio.*, *1*, 77-91, 1995a.
Schimel, D.S., Terrestrial Biogeochemical Cycles: Global Estimates with Remote Sensing, *Remote Sens. Environ.*, *51*, 49-56, 1995b.
Schimel, D.S., B.H. Braswell, R. McKeown, D.S. Ojima, W.J. Parton, and W. Pulliam, Climate and nitrogen controls on the geography and time scales of terrestrial cycling, *Global Biogeochemical Cycles*, *10*, 677-692, 1997.
Scholes, R., The global soil task, *IGBP Newsletter*, *27*, 10, 1996.
Sellers, P., Canopy reflectance, photosynthesis and transpiration, *International Journal of Remote Sensing*, *6*, 1335-1372, 1985.
Sellers, P., Canopy reflectance, photosynthesis and traspiration II. The role of biophysics in the linearity of their interdependence, *Remote Sensing of Environment*, *21*, 143-83, 1987.
Sellers, P., D. Randall, and G. Collatz, A revised land surface parameterization (SiB2) for atmospheric GCMs. Part I: Model formulation, *J. Clim.*, *9*, 676-705, 1996a.
Sellers, P., C. Tucker, G. Collatz, S. Los, C. Justice, D. Dazlick, and D. Randall, A revised land surface parameterization (SiB2) for atmospheric GCMs. Part II: The generation of global fields of terrestrial biophysical parameters from satellite data, *J. Clim.*, *9*, 706-737, 1996b.
Sellers, P.J., C.J. Tucker, G.J. Collatz, S.O. Los, C.O. Justice, D.A. Dazlich, and D.A. Randall, A global 1 degree by 1 degree NDVI data set for climate studies. Part 2: The generation of global fields of terrestrial biophysical parameters from the NDVI, *Int.J. Remote Sensing*, *15*, 3519-3545, 1994.
Spangler, W., and R.L. Jenne, World Monthly Surface Station Climatology, NCAR Computing Facility, 1990.
Stephenson, N.L., Climatic Control of Vegetation Distribution-The Role of the Water Balance, *American Naturalist*, *135*, 649-670, 1990.
Turner, B.L., D.L. Skole, S. Anderson, G. Fischer, L. Fresco, and R. Leemans, Land Use and Land-Cover Change: Science/Research Plan, *IGBP*, *35*, 1995.
Walter, H., and S.-W. Breckle, *Spezielle Okologie der Tropischen und Subtropischen Zonen*, Okologie der Erde, 2, , Gustav Fischer Verlag, Stuttgart, 1983.
Warnant, P., L. Francois, D. Strivay, and J. Gerard, CARAIB: a global model of terrestrial biological productivity., *Global Biogeochemical Cycles*, *8*, 255-270, 1994.
Webb, R., C. Rosenzweig, and E. Levine, A global data set of soil particle size properties in: Global Ecosystems Database Version, NOAA NGDC, Boulder, 1992.
Whittaker, R.H., G.E. Likens, and H.Lieth, Scope and purpose of this volume, *Primary Production of the Biosphere*, *14*, 3-5, 1975.
Wilson, M., and A. Henderson-Sellers, A global archive of land cover and soils data for use in general circulation models., *J. Climate*, *5*, 119-143, 1985.
Woodward, F.I., T.M. Smith, and W.R. Emanuel, A global land primary productivity and phytogeography model, *Global Biogeochemical Cycles*, *9*, 471-490, 1995.
Zinke, P., A. Stangenberger, W. Post, W. Emanuel, and J. Olson, Worldwide Organic Soil Carbon and Nitrogen Data, Oak Ridge National Laboratory, Oak Ridge, 1984.
Zobler, L., A World Soil File For Global Climate Modelling, Goddard Institute for Space Studies, 1986.